Contents

Welcome

Welcome to Galway and to the 6th Annual UK and Ireland SIAM Student Chapter Conference.

Our chapter was founded in September 2014. Echoing SIAM's mission, our goal has been to facilitate interdisciplinary collaboration between students from different disciplines, including mathematics, applied mathematics, statistics, computer science, engineering, economics, physics and other sciences. To work towards that goal, we held our first conference in December 2014. That meeting has now become an annual event, most recently hosted by our good friends at the University of Limerick.

The success of these meetings has led to our Chapter hosting this conference, the first time the SIAM Chapter 'national' conference has been held on the island of Ireland. We are delighted to welcome fifty participants from seventeen institutions, and look forward to a day packed with interesting presentations, and great opportunities to share ideas and discoveries.

We would like to thank our invited guests, Léa Deleris, Patrick Farrell, and Sinéad Burke for so readily agreeing to participate. We are grateful to the support staff of the School of Mathematics, Statistics and Applied Mathematics for their assistance.

We also acknowledge the financial support we have received from the Irish Mathematical Society, NUI Galway's MathSoc, the Stokes Cluster, but, most especially, our primary sponsors Science Foundation Ireland and the UKIE section of SIAM.

We hope you enjoy your time in Galway, and we look forward to seeing you again soon at another SIAM event.

Organising Committee:
Paul Greaney (Chapter President)
Christine Marshall (Chapter Vice-President)
Eoghan Staunton (Chapter Secretary)
Robert Mangan (Chapter Treasurer)
Niall Madden (Faculty Advisor)
Faiza Alssaedi
Richard Burke
Hannah Conroy Broderick
Roberto Galizia
Róisín Hill
Vinh Mai
Cian O'Brien
Qays Shakir
Michael Welby

Schedule

9:15-9:50 Registration & Poster Setup (Arts Millennium Building Foyer)

9:50-10:00 Introduction & Welcome (AM200)

Dr Michael Carty, Vice-Dean for Graduate Studies, College of Science

10:00-10:45 Plenary Lecture 1

Léa Deleris: Taking Decision Making to the Next Level

10:50-11:30 Parallel Talks

	AM200	**AM150**
	Chair: Robert Mangan	Chair: Roberto Galizia
10:50	Alex Mackay	Joshua Duley
	Numerical Simulations of Compressible Non-isothermal Viscoelastic Flow	Random Sequential Adsorption and Dissolution Modelling Heterogeneous Nucleation
11:10	Scott Morgan	Denis Patterson
	Stability of Oscillatory Rotating-Disk Boundary Layers	Blow-up and Asymptotic Growth in Volterra Equations

11:30-12:00 Coffee (Arts Millennium Building Foyer)

12:00-12:40 Parallel Talks

AM200	**AM150**
Chair: Eoghan Staunton	Chair: Hannah Conroy Broderick
Danny Groves	Francisco de Melo Virissimo
Contact Line Dynamics over Heterogeneous Substrates with Mass Transfer	Multilayered Flows in the Shallow-water Limit: Formulation and Stability
Aisling McGlinchey	Shane Walsh
Differential Privacy and the l_1 Sensitivity of Positive Linear Observers	Perturbation Expansion of the Detuned Triad Equations

12:45-13:15 Round-table discussion on Careers in Mathematical Science (AM200)

Chair: Sinéad Burke, MACSI, University of Limerick

13:15-14:45 Lunch & Poster Session (Arts Millennium Building Foyer)

14:45-15:45 Parallel Talks

AM200	**AM150**
Chair: Qays Shakir	Chair: Cian O'Brien
James Fannon	Aleksandar Senek
Numerical Simulations of Drumlin Formation	Multiscale Stochastic Neuron modeling - with Applications in Deep Brain Stimulation
Chun Xie	Craig Gilmour
Rate-induced Critical Transitions	Self-Exciting Point Processes for Crime
Alexander Safar	Niall McInerney
Debonding of Cellular Structures Under Shear Deformation	Mathematical Modelling of a Thermoresponsive Drug Delivery Device

15:45-16:15 Coffee (Arts Millennium Building Foyer)

16:15-17:00 Plenary Lecture 2 - Patrick Farrell (AM200)

Patrick Farrell: Scalable Bifurcation Analysis of Nonlinear Partial Differential Equations

17:00-17:15 Closing Remarks

18:00 Barbecue in the College Bar

Plenary Talks

Taking Decision Making to the Next Level

Lea A. Deleris

IBM Research -Ireland
Mulhuddart, Dublin 15, Ireland

lea.deleris@ie.ibm.com

To a large extent, decision support remains the domain of specialists. While academia has made significant progress in modeling and solving complex decision situations, the general population is no closer to making use of such solutions in business and personal decisions, except when the problem faced neatly matches an existing template.

Why are decisions challenging? Decisions represent a key activity of our daily lives and yet there remain ample room for improvement in the way we approach them. As Kahneman explains [1], many decisions are controlled by our reactive system (which he calls system 1 thinking) where our minds tend to go for the simplest answer, the intuitively and seemingly coherent one. Even when we consciously seek to approach a decision rationally (soliciting what Kahneman calls our system 2), we are affected by human shortcomings such as searching systematically for information, dealing with uncertainty, expressing preferences, dealing with combinatorial options and feedback effects, carrying on complex computations. All those represent tasks where humans are not extremely efficient. Machines, however, and more specifically cognitive systems, can be helpful in completing those tasks and assist us in our decision making process.

In this presentation, through two examples from IBM Research [2, 3], I will illustrate how applied interdisciplinary research, leveraging advances in artificial intelligence broadly defined, can provide solutions to bridge the gap between theory and practice and eventually bring rigorous decision making to the masses.

References

[1] D. Kahneman, *Thinking, Fast and Slow*. New York: Farrar, Straus and Giroux, 2011.

[2] N.Slonim, E. Aharoni, C. Alzate Perez, R. Bar-Haim, Y. Bilu, L. Dankin, I. Eiron, D. Hershcovich, S. Hummel, M. M. Khapra, T. Lavee, R. Levy, P. Matchen, A. Polnarov, V.C. Raykar, R. Rinott, A. Saha, N. Zwerdling, D. Konopnicki and D. Gutfreund, Claims on demand - an initial demonstration of a system for automatic detection and polarity identification of context dependent claims in massive corpora. in: Proceedings of COLING (Demos), 6-9, 2014.

[3] D. Bhattacharjya, and J.O. Kephart, Bayesian Interactive Decision Support for Multi-Attribute Problems with Even Swaps, in: Proceedings of UAI, 72-81, 2014.

Scalable Bifurcation Analysis of Nonlinear Partial Differential Equations

Patrick E. Farrell[†], C. H. L. Beentjes, Á. Birkisson

Mathematical Institute, University of Oxford, Oxford, UK

[†]patrick.farrell@maths.ox.ac.uk

Computing the solutions u of an equation $f(u, \lambda) = 0$ as a parameter $\lambda \in \mathbb{R}$ is varied is a central task in applied mathematics and engineering. In this talk I will present a new algorithm, deflated continuation, for this task [2].

Deflated continuation has three main advantages. First, it is capable of computing disconnected bifurcation diagrams; previous algorithms only aimed to compute that part of the bifurcation diagram continuously connected to the initial data. Second, its implementation is extremely simple: it only requires a minor modification to any existing Newton-based solver. Third, it can scale to very large discretisations if a good preconditioner is available.

Among other problems, we will apply this to a famous singularly perturbed ODE, Carrier's problem. The computations reveal a striking and beautiful bifurcation diagram, with an infinite sequence of alternating pitchfork and fold bifurcations as the singular perturbation parameter tends to zero. The analysis yields a novel and complete taxonomy of the solutions to the problem, and demonstrates that a claim of Bender & Orszag [1] is incorrect.

Acknowledgement. This research was supported by EPSRC grant EP/K030930/1.

References

[1] C. M. Bender and S. A. Orszag, *Advanced Mathematical Methods for Scientists and Engineers I: Asymptotic Methods and Perturbation Theory*, Springer, 1999.

[2] P. E. Farrell, C. H. L. Beentjes, and Á. Birkisson, *The computation of disconnected bifurcation diagrams*, 2016. arXiv:1603.00809 [math.NA].

Student Talks

Numerical Simulations of Compressible Non-isothermal Viscoelastic Flow

Alex Mackay[†], Tim Phillips

School of Mathematics, Cardiff University,
Senghennydd Road, Cardiff CF24 4AG, UK

[†]mackaya1@cardiff.ac.uk

Compressible and non-isothermal effects are often ignored when modelling flows of non-Newtonian fluids[2][4][1]. The additional equations governing density and temperature transport increase the complexity of the governing system of nonlinear partial differential equations which adds to the challenge of devising efficient and stable numerical schemes.

Taylor-Galerkin pressure correction schemes coupled with Discrete Elastic Viscous Stress Splitting (DEVSS) stabilisation enable accurate solutions to be generated for a wide range of viscosities and relaxation times[3]. The derivation of the governing equations is described and some numerical results on benchmark problems are presented. In particular, the flow between eccentrically rotating cylinders (the journal bearing problem) is considered for a range of relaxation times and the influence of compressibility and viscoelasticity on torque and load bearing capacity is assessed.

Governing equations of compressible & nonisothermal viscoelastic flow:

$$\begin{aligned} \rho Re\frac{D\mathbf{u}}{Dt} &= -\nabla p + \left[\beta_s(\theta)\left(\nabla^2\mathbf{u} + \frac{1}{3}\nabla(\nabla\cdot\mathbf{u})\right) + \nabla\cdot\boldsymbol{\tau}_p\right] + \mathbf{F} \\ \frac{\partial\rho}{\partial t} + \nabla\cdot(\rho\mathbf{u}) &= 0 \\ \rho\frac{D\theta}{Dt} &= Di\nabla^2\theta + V_{h^1}\mathbb{T} : \nabla\mathbf{u} - V_{h^2}p\nabla\cdot\mathbf{u} \\ \boldsymbol{\tau}_p + We\psi(\theta)(\overset{\triangledown}{\boldsymbol{\tau}}_p + (\nabla\cdot\mathbf{u})\boldsymbol{\tau}_p) &= 2\psi(\theta)(1-\beta_s)\mathbb{D} \\ \frac{\partial\rho}{\partial p} &= \frac{1}{c_0(\theta)^2} \end{aligned} \tag{1}$$

References

[1] Peter Charles Bollada and Timothy Nigel Phillips. On the effects of a compressible viscous lubricant on the load-bearing capacity of a journal bearing. *International Journal for Numerical Methods in Fluids*, 55(11):10911120, 2007.

[2] Peter Charles Bollada and Timothy Nigel Phillips. On the mathematical modelling of a compressible viscoelastic fluid. *Archive for Rational Mechanics and Analysis*, 205(1):126, 2012.

[3] Susanne Claus. *Numerical simulation of complex viscoelastic flows using discontinuous galerkin spectral/hp element methods*. PhD thesis, Cardiff University, 2013.

[4] D Rh Gwynllyw, AR Davies, and TN Phillips. On the effects of a piezoviscous lubricant on the dynamics of a journal bearing. *Journal of Rheology* (1978-present), 40(6):1239–1266, 1996.

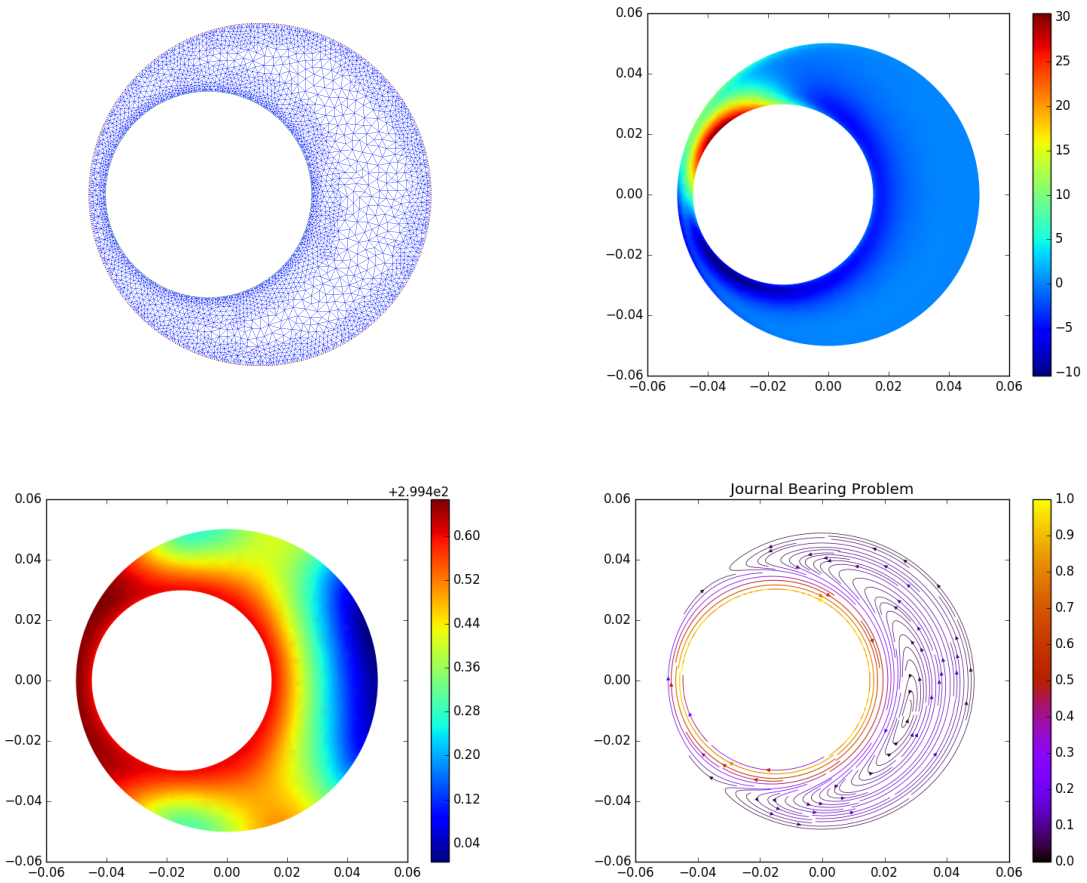

Figure 1: Solutions for the field divergence, temperature and velocity of a compressible viscoelastic lubricant between to eccentrically rotating cylinders: $R_J = 0.03m$, $R_B = 0.05m$, $e = 0.75$ $Re = 200$, $We = 15$

Stability Of Oscillatory Rotating-Disk Boundary Layers

Scott Morgan[†], Christopher Davies

School of Mathematics, Cardiff University
Senghennydd Road, Cardiff, CF24 4AG

[†]MorganSN@cardiff.ac.uk

The rotating disk boundary layer has long been considered as providing an archetypal model for studying the stability of three-dimensional boundary-layer flows. It is one of the few truly three dimensional configurations for which there is an exact similarity solution of the Navier-Stokes equations. The crossflow inflexion point instability mechanism is common to both the rotating disk boundary layer and the flow over a swept wing. Thus the investigation of strategies for controlling the behaviour of disturbances that develop in the rotating disk flow may prove to be helpful for the identification and assessment of aerodynamical technologies that have the potential to maintain laminar flow over swept wings.

We will consider the changes in the stability behaviour that arise when the rotating disk base-flow configuration is altered by imposing a periodic modulation in the rotation rate of the disk surface. This modulation is utilised in order to induce a small level of oscillatory flow into the otherwise steady boundary layer. In effect, a time-periodic oscillatory Stokes layer is added, which has an alignment along the circumferential flow-direction. Thomas et. al. [2] have previously demonstrated that Tollmien-Schlichting waves can be stabilised when a similarly induced Stokes layer is conjoined to a plane channel flow.

Preliminary results indicate that the addition of a temporally oscillatory component to the rotating disk boundary layer can lead to significant stabilising effects, over a range of the parameters that have so far been considered. Current work encompasses three distinct investigatory approaches. Linearised direct numerical simulations have been conducted, using the vorticity-based methods that were first adopted by Davies & Carpenter [1]. These simulations are complemented by a local in time linear stability analysis, that is made possible by imposing an artificial frozen base-flow approximation. This localised analysis is deployed together with a more exact global treatment based upon Floquet theory, which avoids the need for any simplification of the temporal dependency of the base-flow.

With laminar flow control techniques and suppression of crossflow vortices on swept wings foremost in mind, we will focus our presentation on the favourable results that have been discovered for stationary forms of disturbance.

References

[1] C. Davies and P. W. Carpenter, *A novel velocity-vorticity formulation of the Navier- Stokes equations with applications to boundary layer disturbance evolution*, Journal of Com- putational Physics, 172 (2001), pp. 119 – 165.

[2] C. Thomas, A. P. Bassom, P. J. Blennerhassett, and C. Davies, *The linear stability of oscillatory poiseuille flow in channels and pipes*, Proceedings of the Royal Society of London A: Mathematical, Physical and Engineering Sciences, (2011).

Random Sequential Adsorption and Dissolution Modelling Heterogeneous Nucleation

J.M. Duley[1], A.C. Fowler[1 , 2], I. Moyles[1], S.B.G. O'Brien[1]

[1] MACSI, Department of Mathematics and Statistics, University of Limerick, Ireland.

[2] OCIAM, Mathematical Institute, University of Oxford, Oxford, United Kingdom.

joshua.duley@ul.ie; fowler@maths.ox.ac.uk

iain.moyles@ul.ie; stephen.obrien@ul.ie

Nucleation is often assumed to occur instantaneous or at some constant rate without much consideration. However in the context of a wider dynamical system an assumption of instantaneous nucleation can generate discontinuities and render the system unsolvable. Indeed while attempting to model the natural phenomenon of Liesegang rings[1] such a difficulty arose leading to the sub problem presented here.

Considering heterogeneous nucleation of crystal onto a large flat impurity we develop a problem of stochastic geometry whereby monomers adsorb to the surface and experience subsequent growth both by means of a simple stochastic process. In addition to adsorption molecules may indeed dissolve from the surface and so the problem might be categorised as one of random sequential adsorption and dissolution [RSAD]. For sparse coatings we see little interaction of these polymers however as the density is increased we need justify a probabilistic aggregation rate.

In this talk we proceed from a set of Monte-Carlo simulations generating a data set ready to validate the results of the modelling process as well as clarifying the fundamental system. The simulations are executed for both two dimensional bulbous crystals as well as an approximation to one dimensional expressions for crystal size. With the correct observations on our driving mechanisms the system is estimate by a discrete difference equation [2]. While informative the large system of equations this gives is relatively intractable given the original desire for macroscopic descriptions. It is then necessary to reduce the system further to a low dimensional set of ODE's on fractional covering and total number of clusters. Solutions and macroscopic implications included.

References

[1] J.B. Keller, S.I. Rubinow, Recurrent Precipitation and Liesegang Rings. *J. Chem. Phys.* 74(9):5000-5007, 1981.

[2] E, Ben-Naim, P.L. Krapivsky, Nucleation and Growth in one Dimension. *Physical Review E* 54(4):3562-3568, 1996.

[3] A, Rnyi, On a One-Dimensional Problem Concerning Random Space-Filling. *Publ. Math. Inst. Hung. Acad. Sci.* 3: 109-127, 1958.

Blow–up and Asymptotic Growth in Volterra Equations

Denis Patterson†, John Appleby

School of Mathematical Sciences, Dublin City University, Glasnevin, Dublin, Ireland.

†denis.patterson2@mail.dcu.ie

Nonlinear Volterra integral equations of the form

$$x(t) = \int_0^t W(t-s)f(x(s))\,ds + H(t), \quad t \geq 0, \tag{2}$$

arise naturally in the modelling of combustion in a reactive–diffusive medium – typically in the analysis of models based on parabolic PDEs. In this context, f captures the reactivity of the medium and the energy entering the system, W the ability of the medium to diffuse energy, and H the initial data of the problem. If the energy entering the system is not dissipated sufficiently quickly there will be an explosion, both physically and mathematically speaking. Mathematically, finite–time explosion of solutions is possible because physical considerations dictate that the nonlinearity, f, obeys $f(x)/x \to \infty$ as $x \to \infty$.

Both theoretically and practically, the most important questions in relation to (2) are:

(i.) Under what conditions do solutions blow–up?

(ii.) At what time do solutions blow–up?

(iii.) What is the asymptotic behaviour of solutions?

This talk concerns work towards a comprehensive answer to (iii.). Existing asymptotic results for general nonlinearities are either not sharp (e.g. [2, 3]), or not fully rigorous (e.g. [4]). However, some sharp results are available for special classes of nonlinearities and kernels [1]. We present results for a class of nonlinear Volterra equations which illustrate how constructive comparison techniques reduce the analysis of (2) to that of related ODEs. This approach leads to sharp asymptotic results and also recovers well–known necessary and sufficient blow–up criteria in the process.

Acknowledgement. The first author is supported by the Irish Research Council grant GOIPG/2013/402.

References

[1] V. Evtukhov and A. Samoilenko, Asymptotic representations of solutions of nonautonomous ordinary differential equations with regularly varying nonlinearities, *Differential Equations*, 47(5):627–649, 2011.

[2] W. Mydlarczyk, A condition for finite blow-up time for a Volterra integral equation, *Journal of Mathematical Analysis and Applications*, 181(1):248 – 253, 1994.

[3] W. Mydlarczyk, W. Okrasiński, and C. A. Roberts, Blow-up solutions to a system of nonlinear Volterra equations, *Journal of Mathematical Analysis and Applications*, 301(1):208–218, 2005.

[4] C. A. Roberts and W. Olmstead, Growth rates for blow-up solutions of nonlinear Volterra equations, *Quarterly of Applied Mathematics*, 54(1):153–159, 1996.

Contact Line Dynamics over Heterogeneous Surfaces with Mass Transfer

Danny Groves[†], Dr Nikos Savva, Dr Usama Kadri

Cardiff University, School of Mathematics
Senghennydd Road, Cardiff, Wales

[†]GrovesD2@cardiff.ac.uk

Introduction

The contact line dynamics of two and three dimensional droplets spreading over chemically heterogeneous substrates are considered. Assuming small slopes and strong surface tension effects, a long wave expansion of the Stokes equations leads to a single evolution equation (3) for the droplet height where a contact line singularity is removed using a slip condition.

$$\frac{\partial h}{\partial t} + \boldsymbol{\nabla} \cdot (h(h^2 + \lambda^2)\boldsymbol{\nabla}\nabla^2 h) = q(\mathbf{x}, t) \tag{3}$$

Under a quasi-static regime we investigate cases where we have mass transfer through the substrate by controlling the parameter q; modelling absorption or perhaps a needle piercing the droplet base.

Asymptotic Expansions

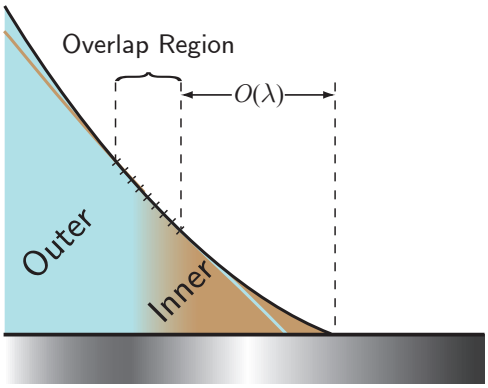

Under the quasi-static limit, we follow approaches similar to that of Hocking [1] in the matched asymptotic analysis. During this process we probe into the dynamics of the outer region where the motion is dominated by capillary forces, and the inner region where slip (λ) is a more predominant force. Obtaining solutions in each domain, we combine the solutions in a process called matching, which is performed in an overlap region sandwiched between the inner and outer regions. While simultaneously studying the physical effects of spreading through the theoretical analysis, an ordinary differential equation system is discovered which quickly and accurately approximates the solution to the full partial differential equation.

Numerical Calculation

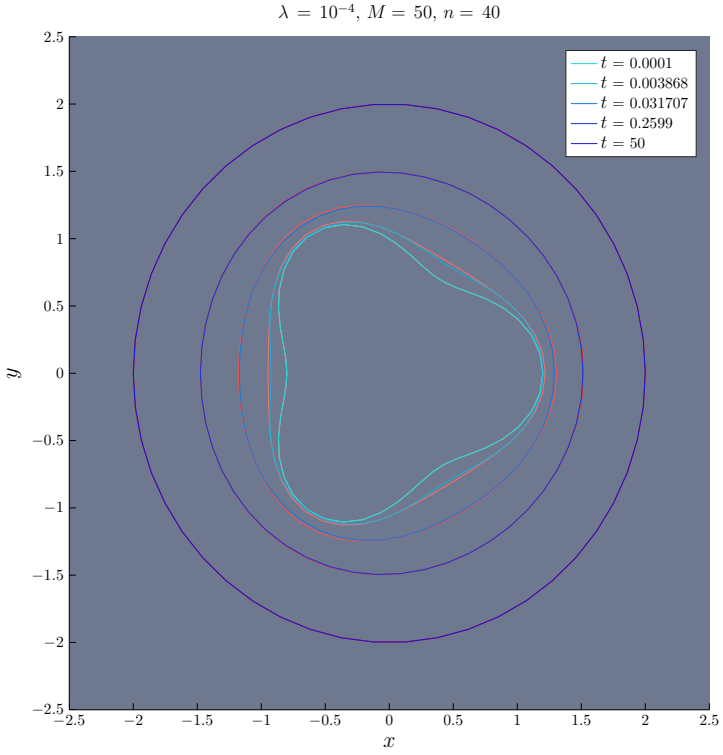

In order to properly test the theoretical approach, a numerical approach based on the methods presented in Trefethen's book '*Spectral Methods in MATLAB*' [2] is utilised. Discretisation in space is achieved using a n point Chebyshev Gauss-Radau grid, where points are mapped towards the boundary for highly accurate solutions, and, in the azimuthal direction M Fourier points are taken. Integration over time is performed using MATLAB's `ode15s` routine. As well as offering a test of validity for the asymptotic analysis, this method also provides us with a chance of observing non quasi-static dynamics on spreading where the asymptotics are not valid.

References

[1] L. M. Hocking. The spreading of a thin drop by gravity and capillarity. *The Quarterly Journal of Mechanics and Applied Mathematics*, 36(1):55-69, 1983.

[2] L. N. Trefethen. *Spectral Methods in MATLAB*, volume 10. SIAM, 2000.

Differential Privacy and the l_1 Sensitivity of Positive Linear Observers

Aisling McGlinchey[†1], Oliver Mason[2]

[1]Dept. of Mathematics and Statistics, Maynooth University, Maynooth, Co. Kildare, Ireland & Lero, the Irish Software Research Centre

[2]Dept. of Mathematics and Statistics/Hamilton Institute, Maynooth University, Maynooth, Co. Kildare, Ireland & Lero, the Irish Software Research Centre

[†]aisling.mcglinchey@nuim.ie

This talk & poster describes work to be presented at the 2017 IFAC World Congress.

We study the problem of designing differentially private observers for positive linear systems in discrete time. In particular, we provide a general bound for the l_1 sensitivity of the map defined by a Luenberger observer for a linear time invariant (LTI) system. We also define an optimisation problem for minimising this bound for positive linear observers and characterise optimal solutions for systems with a single measured output.

First we consider systems of the form:

$$\begin{aligned} x(k+1) &= Ax(k) \\ y(k) &= Cx(k) \end{aligned} \tag{4}$$

where $A \in \mathbb{R}^{n\times n}$, $C \in \mathbb{R}^{p\times n}$. To design a Luenberger observer for this system requires a matrix $L \in \mathbb{R}^{n\times p}$ such that the solution $z(\cdot)$ of the system $\mathcal{L}$ given by

$$\begin{aligned} z(k+1) &= Az(k) + L(y(k) - Cz(k)) \\ &= (A - LC)z(k) + Ly(k) \end{aligned} \tag{5}$$

satisfies $\|z(k) - x(k)\| \to 0$ as $k \to \infty$ where x is the solution of (4).

We wish to release a noisy observer $\hat{z}$ such that the mapping $y \to \hat{z}$ is differentially private, as the signal y contains sensitive personal information.

An ϵ differentially private mechanism can be defined by adding *iid* noise generated from the Laplace distribution with parameter $b = \frac{\Delta(\mathcal{L})}{\epsilon}$ to each component of each $z(k)$ ([4]). $\Delta(\mathcal{L})$ is the l_1 sensitivity of the observer (5) mapping y to z; we define this now.

Definition 0.1 *The l_1 sensitivity $\Delta(G)$ of a system G is defined as*

$$\Delta(G) := \sup_{y\sim y'} \|G(y) - G(y')\|. \tag{6}$$

The following result bounds the l_1 sensitivity of (5).

Proposition 0.1 *Let $A \in \mathbb{R}^{n\times n}$, $C \in \mathbb{R}^{p\times n}$, $L \in \mathbb{R}^{n\times p}$ be given and suppose that $\|A - LC\| < 1$. Consider the Luenberger observer, $\mathcal{L}$ given by* (5)*. Then for an adjacency relation, the l_1 sensitivity of $\mathcal{L}$ (as given in (6)) is bounded by*

$$\Delta(\mathcal{L}) \leq \left(\frac{K}{1-\alpha}\right)\left(\frac{\|L\|}{1-\|A-LC\|}\right). \tag{7}$$

Positive systems arise in areas such as epidemiology and social network analysis. It is natural to require that an observer for a positive system respects the positivity property for all signals ([1, 3, 2]). This makes the problem of *positive observer design* distinct to classical observer.

K and α are determined by relation $\sim$ and the bound given by (7) is valid for L with $\|A - LC\| < 1$. We propose the following general problem.

Problem 0.1 *Given* $A \in \mathbb{R}_+^{n\times n}$, $C \in \mathbb{R}_+^{p\times n}$, ***minimise***

$$F(L) := \frac{\|L\|}{1 - \|A - LC\|} \tag{8}$$

subject to the constraints:

$$LC \geq 0 \ , \ A - LC \geq 0, \ \|A - LC\| < 1 \tag{9}$$

For the case of a single output system so that $C \in \mathbb{R}^{1\times n}$, minimising the l_1 sensitivity bound (7) reduces to the following uni-variate constrained optimisation problem, where $x = \|L\| = \sum_{i=1}^n l_i$, as $L \in \mathbb{R}^{n\times 1}$ is the usual l_1 norm of the associated column vector.

Problem 0.2 ***Minimise***

$$f(x) = \max_j \frac{x}{(1 - \sum_{i=1}^n a_{ij}) + c_j x}$$

subject to

$$x \geq 0 \,\&\, \max_j \frac{1}{c_j}\left(\sum_{i=1}^n a_{ij} - 1\right) < x \leq \sum_{i=1}^n \min_j \frac{a_{ij}}{c_j}$$

Define $f_j(x) = \frac{x}{(1-\sum_{i=1}^n a_{ij})+c_j x}$, $1 \leq j \leq n$. There are 3 case to consider in this problem: (i) all f_j are concave; all f_j are convex; (ii) mixed case of both concave and convex. For each of these cases, we have developed a graphical and analytical method for solve for x.

Acknowledgement. This work was supported with the financial support of the Science Foundation Ireland grant 13/RC/2094 and co-funded under the European Regional Development Fund through the Southern & Eastern Regional Operational Programme to Lero - the Irish Software Research Centre (www.lero.ie).

References

[1] M. Ait Rami and F. Tadeo, *Positive observation problem for linear discrete positive systems*, Proc. IEEE 45th Annual Conference on Decision and Control (CDC), (2006).

[2] J. Back and A. Astolfi, *Design of positive linear observers for positive linear systems via coordinate transformations and positive realizations*, SIAM J. Control & Opt., 47 (2008), pp. 345–373.

[3] H. Hardin and J. van Schuppen, *Observers for linear positive systems*, Lin. Alg. and its Appl., 425 (2007), pp. 571–607.

[4] J. Le Ny and G. Pappas, *Differentially private filtering*, IEEE Tran. Aut. Cont., 59 (2014), pp. 341–354.

Multilayered Flows in the Shallow-water Limit: Formulation and Stability

Francisco de Melo Viríssimo[†], Paul A. Milewski

Department of Mathematical Sciences, University of Bath,
Claverton Down Road, Bath, Somerset, UK

[†]F.de.Melo.Virissimo@bath.ac.uk

In this talk, we will formulate and discuss the problem of density stratified interfacial flows in the shallow-water limit. This type of flow occurs in nature with the atmosphere and ocean as prime examples [7], [3].

Mathematical studies of these are particularly important, since wave motion tends not to be resolved by most numerical climate models due to their fast scales, and thus need to be understood and parameterized [6]. For example waves may break and dissipate energy or mix the underlying fluids and affect the very medium in which they are propagating [8], [5]. Consequently this research will both increase the understanding of internal waves, and have an impact on future climate models.

We will focus our attention on the two and three-layer flows, without the so-called *Boussinesq approximation* which requires small density differences. This is a simplified model for geophysical situations, but it is not too simplified: the model has both *barotropic* (fast waves affecting the whole fluid uniformly) and *baroclinic* modes (slower waves with more internal structure) [2].

The governing equations will be derived and the dynamics of their solutions will be studied from both analytical and numerical points of view, particularly the issue of whether the solutions maintain hyperbolicity (i.e. wave-like behaviour) [4], [1].

Acknowledgements. This research is supported by CNPq (Conselho Nacional de Desenvolvimento Científico e Tecnológico, Brasil), grant number 249770/2013-0, to whom the authors are grateaful. FdMV and PAM also want to thank the Department of Mathematical Sciences at the University of Bath, where this work is being developed.

References

[1] A. Boonkasame and P. A. Milewski, The stability of large-amplitude shallow interfacial non-Boussinesq flows. *Stud. in Appl. Math.* 128:40-58, 2011.

[2] L. Chumakova, F. A. Menzaque, P. A. Milewski, R. R. Rosales, E. G. Tabak and C. T. Turner, Stability properties and nonlinear mappings of two and three layer stratified flows. *Stud. in Appl. Math.* 122:123-137, 2009.

[3] B. Cushman-Roisin and J-M.Beckers, *Introduction to Geophysical Fluid Mechanics - Physical and Numerical Aspects*. Academic Press, Waltham, Second edition, 2011.

[4] P. A. Milewski, E. G. Tabak, C. T. Turner, R. R. Rosales and F. A. Menzaque, Nonlinear stability of two-layer flows. *Comm. Math. Sci.* 2:427-442, 2004.

[5] P. A. Milewski and E. G. Tabak, Conservation law modelling of entrainment in layered hydrostatic flows. *J. Fluid Mech.* 772:272-294, 2015.

[6] J.H. Ritcher, F. Sassi and R. R. Garcia, Toward a physically based gravity wave source parametrization in a general circulation model. *Journal of the Atmospheric Sciences* 67:136-156, 2010.

[7] G. B. Whitham, *Linear and Nonlinear Waves*. Wiley-Interscience, First edition, 1974.

[8] C. B. Whalen, L. D. Talley and J. A. MacKinnon, Spatial and temporal variability of global ocean mixing inferred from Argo profiles. *Geophys. Res. Lett.* 39, 2012.

Perturbation Expansion of the Detuned Triad Equations

Shane Walsh[†], Miguel D. Bustamante

UCD Institute for Discovery
School of Mathematics and Statistics
University College Dublin, Belfield, Dublin 4

[†]shane.walsh.3@ucdconnect.ie

We consider the detuned triad equations which arise from an integrable Hamiltonian three-wave equation [1]. We wish to study the behaviour of these equations in the limit as the detuning parameter, δ, approaches infinity. Our motivation for doing this is to better understand when jumps in the triad phase's precession frequency occur as a function of the detuning parameter, giving us more insight into how precession resonance can occur in nonlinear turbulent wave systems [2]. To study this we perturbatively expand the equations using the method of multiple scales [3]. We do this by identifying the perturbation parameter as $\epsilon = 1/\delta$, and expand the equations up to and including second order in ϵ, to then validate the perturbative solution using numerical simulations of the original equations. We present the following analytical results: a criterion on the amplitudes for a jump in phase precession frequency to occur and a perturbation expansion for the nonlinear frequencies in terms of the amplitudes.

Acknowledgments. Irish Research Council (IRC) for providing funding through The Government of Ireland Postgraduate Scholarship

References

[1] J. Harris (2013), PhD Thesis, Chapter 3, *The kinematics, dynamics and statistics of three-wave interactions in models of geophysical flow.* wrap.warwick.ac.uk/58419/1/WRAP_THESIS_Harris_2013.pdf

[2] M. D. Bustamante, B. Quinn, & D. Lucas (2014), Robust Energy Transfer Mechanism via Precession Resonance in Nonlinear Turbulent Wave Systems. *Physical Review Letters*, 113(8), 084502. doi:10.1103/PhysRevLett.113.084502

[3] Ali H. Nayfeh, *Perturbation Methods.* Wiley Publications, 1st Edition, 1973.

Numerical Simulations of Drumlin Formation

James Fannon[†1], Andrew C. Fowler[1,2], Iain Moyles[1]

[1]MACSI, Department of Mathematics and Statistics,
University of Limerick, Limerick, Ireland
[2]OCIAM, University of Oxford, Oxford, UK

[†]james.fannon@ul.ie

Drumlins can be loosely defined as small oval-shaped hills, generally occurring in large groups, that are found in regions which were once covered by ice sheets. They form part of a wider family of ubiquitous landforms collectively known as "subglacial bedforms", also consisting of ribbed moraine (ribs) and mega-scale glacial lineations (MSGL), whose formation is typically attributed to the motion of ice sheets. Indeed, such bedforms are estimated to account for up to 50% of Ireland's land area [1]. While subglacial bedforms, in particular drumlins, have attracted much scientific interest for well over 100 years [5], few quantitative descriptions elucidating their genesis have been proposed.

We summarise the present form of a mathematical model known as the instability theory of drumlin formation, which describes the coupled flow of ice, subglacial water and sediment. By performing a linear stability analysis of the model equations, one finds that an inherent instability exists such that perturbations to a flat sediment surface can grow exponentially at finite downstream and across-stream wavenumbers [4]. Such growth at preferred wavelengths is compatible with the self-organising behaviour observed in drumlin fields [2]. Preferred wavenumbers are found to vary with a critical parameter such that the instability can naturally account for the formation of ribs and MSGL, providing a possible explanation for the hypothesized continuum of subglacial bedforms [3].

To investigate bedform evolution beyond the initial growth phase, we propose a novel numerical method to solve the model which combines both spectral and finite difference methods. We demonstrate that simulations can be obtained for realistic values of most of the model parameters, with the exception of that corresponding to the water film thickness. Our results indicate that truly three-dimensional bedforms arise with sizes on the order of those observed in nature. One finds that these bedforms continually evolve in time and can resemble ribs, drumlins, and to a lesser extent, lineations.

Acknowledgement. We acknowledge support from Science Foundation Ireland under grant numbers SFI/12/IA/1683 and SFI/13/IA/1923.

References

[1] C.D. Clark, A.L.C. Hughes, S.L. Greenwood, M. Spagnolo and F.S.L. Ng, Size and shape characteristics of drumlins, derived from a large sample, and associated scaling laws. *Quat. Sci. Rev.* 28(7):677-692, 2009.

[2] C.D. Clark, Emergent drumlins and their clones: from till dilatancy to flow instabilities. *J. Glaciol.* 56(200):1011-1025, 2010.

[3] J.C. Ely, C.D. Clark, M. Spagnolo, C.R. Stokes, S.L. Greenwood, A.L.C. Hughes, P. Dunlop and D. Hess, Do subglacial bedforms comprise a size and shape continuum? *Geomorphology* 257:108-119, 2016.

[4] A.C. Fowler and M. Chapwanya, An instability theory for the formation of ribbed moraine, drumlins and mega-scale glacial lineations. *Proc. R. Soc. London, Ser. A* 470(2171), 20140185.

[5] D.E. Sugden and B.S. John, *Glaciers and Landscape*. Edward Arnold, London, 1976.

Rate-induced Critical Transitions

Chun Xie†, Sebastian Wieczorek

School of Mathematical Sciences, University College Cork, Western Road, Cork, Ireland

†chun.xie@ucc.ie

Critical transitions or tipping points are sudden and unexpected changes in the state of a complex system with time-varying external input, which are known to occur in climate[6, 5], engineering[3], biology[2, 1], and etc.

Generally, there are three categories of tipping[4]: bifurcation-induced, noise-induced and rate-induced (R-tipping). This project focuses on R-tipping, where the system fails to follow a moving stable state and undergoes a critical transition but only if the external conditions vary too fast. Mathematically, R-tipping is a genuine nonautonomous instability that cannot be explained by the classical bifurcation theory and requires an alternative approach.

At the first stage of the project, a time compactification method is developed for R-tipping analysis in nonautonomous system with time-varying but asymptotically constant inputs.

Specifically, we consider:

$$\frac{dx}{dt} = f(x, \Lambda(t)), \tag{10}$$

where $x \in \mathbb{R}^n$ describes the state of the system and $\Lambda(t)$ represents the time-varying external input (external forcing) that 'dies out' over time:

$$\lim_{t\to\pm\infty} \Lambda(t) = \lambda_\pm, \ \lim_{t\to\pm\infty} \frac{d\Lambda}{dt} = 0.$$

The system is asymptotically constant in the sense that

$$f(x, \Lambda(t)) \to f(x, \lambda_\pm) \ \text{ as } \ t \to \pm\infty.$$

The main difficulty in the analysis of system (10) is the lack of closed invariant sets such as equilibrium points, limit cycles, or tori. Although such sets do exist at $t = \pm\infty$, system (10) is not defined there.

To overcome this difficulty, we define a suitable compactification of time

$$t = h(s), h : (-1, 1) \to \mathbb{R}, \tag{11}$$

and reformulate nonautonomous system (10) as the **compactified autonomous system**

$$\begin{aligned} \frac{dx}{dt} &= f(x, \Lambda(s)) \\ \frac{ds}{dt} &= \left(\frac{dh}{ds}\right)^{-1} \end{aligned} \tag{12}$$

defined on $\mathbb{R}^n \times [-1, 1]$. By 'suitable compactification' we mean one that satisfies compactification conditions

$$\begin{aligned} &\lim_{s\to\pm1} \frac{d^2h}{ds^2}\left(\frac{dh}{ds}\right)^{-2} \in \mathbb{R} \\ &\lim_{s\to\pm1} \frac{d\Lambda}{ds} = \lim_{s\to1} \frac{d\Lambda}{dh}\frac{dh}{ds} \ \in \mathbb{R} \end{aligned} \tag{13}$$

to ensure that the compactified autonomous system is at least C^1-smooth.

The key feature of the compactified autonomous system are flow-invariant subspaces $s = \pm 1$ which include equilibrium points. This method allows to study the critical rate of change of the time-varying input in terms of a heteroclinic connection between saddle-type invariant sets, which greatly simplifies the analysis. This methodology has been applied to canonical ODE examples of reversible and irreversible R-tipping.

In the next stage, the project will focus on the analysis of R-tipping in agent-based models of terrestrial and aquatic ecosystems.

Acknowledgement. Many thanks to the supervision and help of my supervisor Prof. Wieczorek. The project is supported by the European Union's Horizon 2020 Marie Skłodowska Curie Innovative Training Networks "CRITICS" under Grant Agreement number No.643073.

References

[1] C. Colon, D. Claessen, and M. Ghil, Bifurcation analysis of an agent-based model for predatorprey interactions. *Ecological Modelling* 317: 93-106, 2015.

[2] J. M. Drake and B. D. Griffen, Early warning signals of extinction in deteriorating environments. *Nature* 467: 456459, 2010.

[3] N.A. Alexander, O. Oddbjornsson, C.A. Taylor, H.M. Osinga, and D.E. Kelly, Exploring the dynamics of a class of post-tensioned, moment resisting frames. *Journal of Sound and Vibration* 330: 3710-3728, 2011.

[4] P. Ashwin, S. Wieczorek, R. Vitolo and P. Cox, Tipping points in open systems: bifurcation, noise-induced and rate-dependent examples in the climate system. *Phil. Trans. R. Soc.* 370: 1166-1184, 2012.

[5] T. M. Lenton, H. Held, E. Kriegler, J. W. Hall, W. Lucht, S. Rahmstorf and H. Schellenhuber, Tipping elements in the earth's climate system. *Proc. Natl Acad. Sci.* 105: 1786-1793, 2008.

[6] V. Dakos, M. Scheffer, E. H. van Nes, V. Brovkin, V. Petoukhov and H. Held, Slowing down as an early warning signal for abrupt climate change . *Proc. Natl Acad. Sci.* 105: 14308-14312, 2008.

Debonding of Cellular Structures Under Shear Deformation

Alexander Safar†, Hayley Wyatt and L. Angela Mihai

School of Mathematics, Cardiff University
Senghennydd Road, Cardiff, Wales

†safarat@cardiff.ac.uk

Introduction

Cellular tissues such as apples, pears and potatoes are a collection of fluid filled parenchyma cells bound together by inter-cellular cohesion. In a ripe and juicy apple, fluid is released from cells as the cell wall ruptures (cell bursting). In overripe or cold-stored fruit the strength of the inter-cellular cohesion decreases and the cell wall strength increases, such that it takes less energy to separate cells than to burst [1]. The phenomena of cell separation, or debonding, is key in explaining the behaviour of fruit and legumes during storage or cooking, and is decisive for the quality of food products [1].

Cell properties determine tissue behaviour and applied external forces change the cell responses as deformation progresses [4,5]. These relations lead to nonlinear mechanical behaviour and the requirement for a multi-scale approach. This study uses numerical models to provide evidence of how the cell wall, cell contents and inter-cellular cohesion contribute to cell debonding in soft fruits and tissues. Particular focus is given to shear deformation as this has been largely neglected in literature.

Empty Cells with Unilateral Contact

Using FEBio (Finite Element for Biomechanics) [3], we model periodic structures with hexagonal prismatic cells, subject to horizontal shear. For computational efficiency, we implement the *successive deformation decomposition procedure* (SDDP) proposed in [6]: (i) first, a continuous deformation is computed for the entire the structure (assuming no cell separation); (ii) then, from the pre-deformed structure, the unilateral contact between cell walls are taken into account and cells are able to separate. Results show that, when structures are subject to shear deformation, gaps appear between adjacent cells, causing extensive cell separation diagonally across the structure (Figure 2).

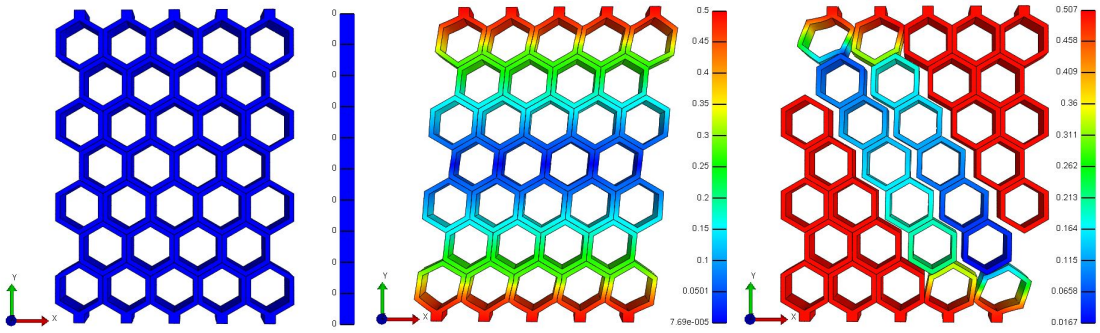

(a) Reference configuration. (b) Continuously deformed state. (c) Current configuration.

Figure 2: SDDP of a 5x7 cellular tissue, subject to shear. Colour indicates total X displacement.

Intercellular Cohesion

Cohesion on a contact interface is usually modelled by the condition $\mathbf{P}(\mathbf{X})\mathbf{N} \cdot \mathbf{N} \leq g$ on Γ_C, where $g > 0$ indicates that a tensile force of magnitude g is permissible whilst two bodies are in contact.

Computationally, this leads to highly unstable systems, so we consider instead an internal cell pressure which is normal to the cell walls and has the same magnitude for each cell. This creates a compressive normal force which must be overcome to separate cell walls, analogous to normal contact cohesion. Results show that a higher surface pressure delays the initiation of inter-cellular gap opening.

Filled Cells

In our study, the influence of the cell inclusions on the inter-cellular contact is addressed by modelling the inclusions as a nearly-incompressible, softer elastic material. A primary effect of this is the cell volume constraint. Results show that the rate of increase in gap size is lower with cell inclusions.

Alternatively, the presence of cell inclusions could be modelled by imposing uniform normal pressure on the internal cell walls. Formally, this is similar to our model for inter-cellular cohesion, suggesting that higher cell pressure results in an increased inter-cellular cohesion.

Conclusion

We model computationally cellular bodies with nonlinear hyperelastic cell walls in mutual non-penetrative contact under large shear deformations, and propose a two-step strategy which we employ to solve the multi-body contact problems more efficiently. Our numerical results are in agreement with physical observations that tissue from overly mature fruit (apple, pear), where cell pressure is low and intercellular cohesion is weak, breaks down into small clumps of undamaged cells, whereas fruit of a lower maturity, with high cell pressure and intercellular cohesion will not debond easily.

References

[1] F.R. Harker, R. Redgwell, I.C. Harlett, and S. Murray. Texture of fresh fruit. *Hortic Rev*, 20, 1997.

[2] F.R. Harker and I.C. Hallett. Physiological changes associated with development of mealiness of apple fruit during cool storage. *Hort Science*, 27(2712):1291-1294, 1992.

[3] S.A. Maas, B.J. Ellis, G.A. Ateshian, and J.A. Weiss. FEBio: Finite elements for biomechanics. *J Biomech Eng*, 134(1):011005, 2012.

[4] L.A. Mihai, K. Alayyash and A. Goriely. Paws, pads, and plants: The enhanced elasticity of cell-filled load-bearing structures. *P ROY SOC LOND A MAT*, 471(2178):0107, 2015.

[5] L.A. Mihai, K. Alayyash and H.L. Wyatt. The optimal density of cellular solids in axial tension. *Comput Methods Biomech Biomed Engin*, 2017.

[6] L.A. Mihai, A. Safar and H.L. Wyatt. Debonding of cellular structures with fibre-reinforced cell walls under shear deformation. *J ENG MATH*, 2017.

Multiscale Stochastic Neuron modeling - With Applications In Deep Brain Stimulation

Aleksandar Senek†, Stefan Engblom

Division of Scientific Computing, Uppsala University, Uppsala, Sweden

†Aleksandar.Senek.1902@student.uu.se

In recent years deep brain stimulation (DBS) has seen success in curing adverse effects of several diseases, among those Parkinson. Current method for treatment uses implanted electrodes in the brain which stimulate neurons [1]. In later years the use of stochastic modeling methods of neurons have attracted some attention as noise is believed to play an important role in the human nervous system [2, 3].

By integrating the cable-equation [4] using a second order scheme and a stochastic model for the ion channels the correct behavior is achieved in the classical limit of a macroscopic neuron. The ion-channel simulation error compared to a reference ODE solution is $\sim 10^{-4}$, for spike train inducting current. The numerical scheme used was Crank-Nicholson and two ion-channels, sodium and potassium, were simulated using a Gillespie SSA algorithm written in C and compiled with MEX. Convergence studies of inter-spike interval (ISI) convergence, as the time step decreases, are presented in Figure 1.

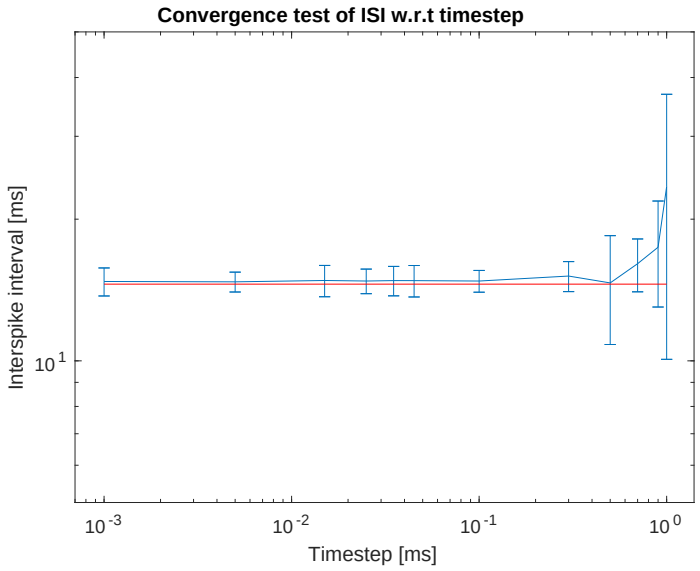

Figure 3: Convergence of ISI for a $1mm$ long cable with a diameter of $1\mu m$. The red line shows the ISI of the ODE model with the same model and parameters. The sample size for each time step is 40. The error-bars show the logarithm of the standard deviations.

Due to the highly parallel nature of the problem the simulation time could be improved through parallelism. The dominating computational time was spent evaluating the stochastic simulation of ion-channels, which is a highly parallel task. As is, the stochastic model requires a factor ~ 10 more time than the classical ODE Hodgkin Huxley model.

In Figure 2 we show that the stochastic model of a neuron has lower threshold current for a potential spike compared to the ODE model. Coupled with the kinetic model of a synapse we create a complete

system allowing for the computation and parametrization of a neural-tissue system and propagation into extra-cellular space.

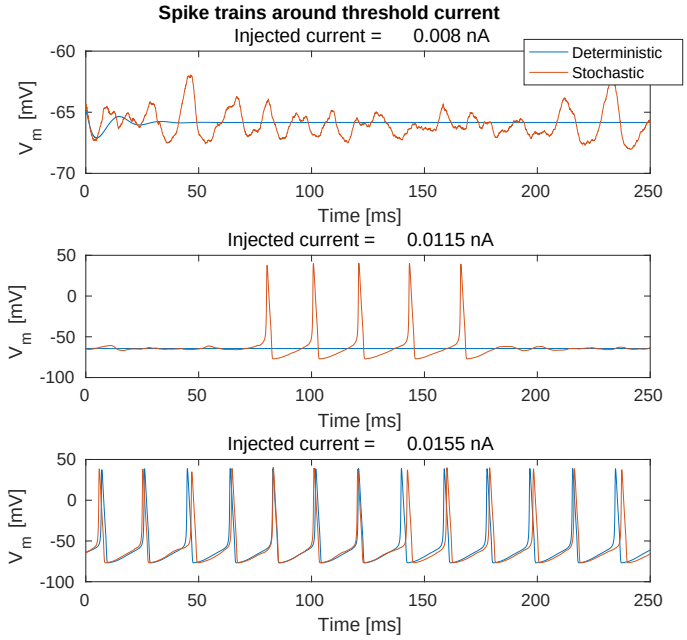

Figure 4: Shows the membrane potential, V_m over time with a constant injected current. The model used was a $1mm$ long cable with a diameter of $1\mu m$.

References

[1] Cubo, R, Medvedev, A, Astrom M, Model-Based Optimization of Individualized Deep Brain Stimulation Therapy, Design & Test IEEE, vol. 33, pp. 74-81, 2016.

[2] Hepburn, I., Chen, W., Wils, S., De Schutter, E. STEPS: efficient simulation of stochastic reaction-diffusion models in realistic morphologies. BMC Systems Biology 2012., 6, 36.

[3] Finke C, Postnova S, Rosa E, Freund JA, Huber MT, Voigt K, Moss FE, Braun HA, Feudel U. Noisy activation kinetics induces bursting in the Huber-Braun neuron model. The European Physical Journal-Special Topics. 2010, 187(1):199-203.

[4] Bauer P, Engblom S, Mikulovic S. Multiscale modeling via split-step methods in neural firing. arXiv preprint arXiv:1611.00509. 2016.

Self-Exciting Point Processes for Crime

Craig Gilmour[†], Des Higham

Department of Mathematics and Statistics, University of Strathclyde
Glasgow, G1 1XH

[†]craig.gilmour@strath.ac.uk

The question of how crime spreads is an important issue for police and society alike, with some crime types displaying highly clustered sequences in time and space. It has been proposed that certain types of crime, such as burglary, gang crime, and gun violence [3, 4], take place in highly clustered event sequences, and therefore can be modelled in much the same way that seismic events are, where earthquakes increase the risk of aftershocks occurring in close proximity to the original earthquake.

Self-exciting point processes can be used in situations where the occurrence of an event increases the chances of a subsequent event happening, and can be defined by their *conditional intensity function*

$$\lambda(t) = \lim_{\Delta t \to 0} \frac{\mathbb{E}(N(t, t+\Delta t)|\mathcal{H}_t)}{\Delta t}, \tag{14}$$

where $\mathcal{H}_t$ is the history of the process prior to t, and $N(t, t+\Delta t)$ describes the number of points observed in an interval after t.

The Hawkes process is a self-exciting point process whose conditional intensity increases in the aftermath of an event [1]. The conditional intensity function can be given as

$$\lambda(t) = \mu + \sum_{t_i < t} g(t - t_i), \tag{15}$$

where we consider μ to be the background rate, and g to be a triggering function which increases the intensity of the process in the aftermath of an event. Traditionally a parametric form of g has been used, e.g. $g(t) = \alpha\omega e^{-\omega t}$ (known as the epidemic type aftershock, or ETAS, model).

In recent years a method called Model Independent Stochastic Declustering (MISD) has been developed, which can find a non-parametric form for the triggering function without any prior assumptions [2]. In this presentation we propose and analyse a new triggering function, and compare its performance against ETAS and non-parametric models. We look at issues of calibration, inference and prediction, and give results on real crime data made publicly available by the Chicago Police Department.

References

[1] A.G. Hawkes, Spectra of Some Self-Exciting and Mutually Exciting Point Processes, *Biomektra*. 58:83-90, 1971.

[2] D. Marsan and O. Lengliné, Extending Earthquakes' Reach Through Cascading, *Science*. 319:1076-1079, 2008.

[3] G.O. Mohler, Marked point process hotspot maps for homicide and gun crime prediction in Chicago, *International Journal of Forecasting*. 30,3:491-497, 2014.

[4] G.O. Mohler, M.B. Short, P.J. Brantingham, F.P. Schoenberg and G.E. Tita, Self-Exciting Point Process Modeling of Crime, *Journal of the American Statistical Association*. 106(493):100-108, 1970.

Mathematical Modelling of a Thermoresponsive Drug Delivery Device

Niall McInerney†, Stephen O'Brien, Sarah Mitchell, Tuoi Vo

MACSI, Department of Mathematics and Statistics, University of Limerick, Limerick, Ireland

†niall.mcinerney@ul.ie

Thermoresponsive polymers can respond drastically to a change in temperature of the environment, which makes them the subject of extensive research with a wide variety of potential applications. In polymers with a lower critical solution temperature (LCST), the polymer undergoes a sharp transition from a swollen, wet, hydrophilic state to a collapsed, dry, hydrophobic state when the polymer is heated above the LCST. Polymers can be synthesised by copolymerising with hydrophilic or hydrophobic monomers to get a desired LCST. In a potential drug delivery device, pulsatile release (fast/slow) can be controlled by cooling/heating of the polymer. Previous modelling work on this subject has only considered instantaneous boundary movements, where the polymer jumps from being in a condensed state to a swollen state with the temperature switch, and thus the properties of the polymer are treated as simple step functions [1].

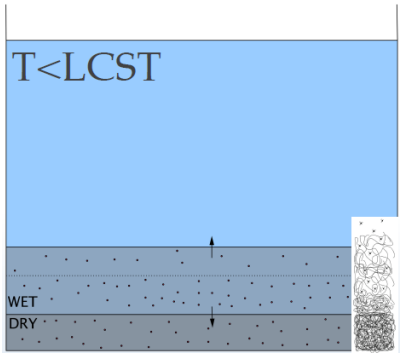

Figure 5: Schematic of a thermoresponsive polymer in contact with a solvent below its LCST.

In this talk we will present the development of a one-dimensional non-linear double moving boundary problem based on the diffusion of a drug from such a device. This model tracks the concentrations of the penetrating solvent from the environment and the drug being released as well as the positions of the swelling/collapsing interface boundary and the boundary separating the wet swollen polymer from the still dry polymer (see Figure 5). We will discuss analytical and numerical results as well as comparisons with experimental data.

References

[1] R.Yang, T.T.N. Vo, A.V. Gorelov, F. Aldabbagh, W.M. Carroll, M.G. Meere, Y. Rochev, A mathematical model for pulsatile release: Controlled release of rhodamine B from UV-crosslinked thermoresponsive thin films. *International journal of pharmaceutics*, 427:320-327, 2012

Posters

Synergy of Data Assimilation and Inverse Problems Techniques

J. Alswaihli[†1], R. Potthast[*1,2], D. Saddy[1]

[1]Department of Mathematics and Statistics, University of Reading,
Whiteknights, PO Box 220, Berkshire RG6 6AX, UK
[2]Deutscher Wetterdienst, Data Assimilation Unit, Frankfurter Str. 135, 63067 Offenbach

[†]j.alswaihli@student.reading.ac.uk
[*]r.w.e.potthast@reading.ac.uk

The need to understand the neural field activity for realistic living systems is a current challenging task in neuroscience. Already for decades, neural fields have been studied and developed theoretically and numerically. However, to make practical use of the equations, we need to *determine their constituents* in practical systems. This includes the determination of parameters or the reconstruction of the underlying connectivity in biological tissue [2, 3, 4, 1, 6] .

In neural dynamics, neurons send electrical spikes to each other within their complicated network structure causing excitation or inhibition. Considering the simple field which is one-dimensional and homogeneous with excitatory and inhibitory neurons, the activity of networks of neurons described by integro-differential equation. This equation is considering several biological mechanism, in general with delay embedded in the firing rate. In reality, the velocity and the time of transmission of the synaptic signals cause such delay. Taking it into account, The delay neural field equation is

$$\tau \frac{\partial u}{\partial t}(r,t) = -u(r,t) + \int_\Omega w(r,r') f(u(r', t - \frac{D(r,r')}{v}))\, dr'. \tag{16}$$

Here $u(r,t)$ interprets a neural field representing the activity of the population of neurons at position r and time t, the second term on the right-hand side represents the synaptic input, with f is the activation (or firing rate) function of a single neuron, with homogeneous kernels $w(r-r')$, which is often referred to as the synaptic footprint or the connectivity function, presents the strength of connection between neurons separated by a distance $|r-r'|$. Normally w represents three different kinds of relations:the connection itself when $w \neq 0$, the different effect either excitation $w > 0$ or inhibition $w < 0$, and the strength of connectivity by $|w|$. Here $D(r,r')$ is the length of the fiber between r and r', and v is the finite propagation speed of signals. For simplify, we will work with $D(r,r') = \|r-r'\|$ and $v = 1$. We study the neural field equation on some bounded domain $\Omega \subset \mathbb{R}^m$ in a space with dimension $m \in \mathbb{N}$. And the initial condition is

$$u(r,t) = u_0(r,t), \quad (r,t) \in \Omega \times [-|\Omega|, T], \tag{17}$$

The research is concerned with two basic tasks in the framework of a *neural field model*.

- the *state estimation* needs to reconstruct the structural information and
- the *reconstruction* needs estimation of the states.

We present an iterative approach to determine both the neural states for simulations and the underlying parameter functions in an iterative procedure which takes in turn the state estimation or data assimilation problem and the inverse neural field problem. We firstly reformulate the inverse problem into a *family of*

integral equations of the *first kind*. Then, we employ a 3D-VAR type algorithm for data assimilation and the approach of Potthast and beim Graben (2009) [5] for solving the inverse problem. We visualize this approach with numerical example in figure 6.

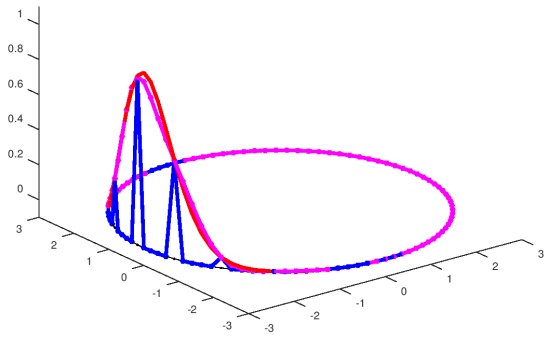

Figure 6: This figure shows the state estimation in one time slide

Our algorithms are built on standard types of medical *measurement data* which are usually functions of the neural excitation fields. For example, an electrode measures the integrated activity of a large number of neurons.

Acknowledgement. First, I am deeply grateful to my sponsor, the Libyan Government. I would also thank Ingo Bojak and Axel Hutt for their feedback and support.

References

[1] F. M. Atay and A. Hutt, Stability and Bifurcations in Neural Fields with Finite Propagation speed and General Connectivity. *SIAM J. Appl. Math.*, , 65 No. 2:644-666, 2005.

[2] P. C. Bressloff and S. Coombes, Physics of the extended neuron *International Journal of Modern Physics B*, 11, 1997.

[3] S. Coombes, P. bbeim Graben, R. Potthast and J. Wright, *Neural Fields: Theory and Applications*. Springer, 2014.

[4] G. Faye and O. Faugeras, Some theoretical and numerical results for delayed neural field equations. *Physica D*, Elsevier, 239:561-578, 2010.

[5] P. beim Graben and R. Potthast, Inverse Problems in Dynamic Cognitive Modeling. *Chaos- An Interdisciplinary Journal of Nonlinear Science*, American Institute of Physics, 2009.

[6] G. Nakamura and R. Potthast, *Inverse Modeling: An introduction to the theory and methods of inverse problems and data assimilation*. IOP Institute of Physics, Bristol, 2015.

An investigation of Systematic Errors in Solar Radiation in Reanalysis Models

Eadaoin Doddy[†1,2], Conor Sweeney[1,2]

[1]UCD Energy Institute, University College Dublin, Ireland
[2]UCD School of Mathematics and Statistics, University College Dublin, Ireland

[†]eadaoin.doddy@ucdconnect.ie

The design and estimation of the performance of any solar energy system requires knowledge of solar radiation data obtained over a long period of time. The use of solar photovoltaic (PV) energy in Ireland is growing, leading to more interest in accurate solar radiation climatology. Reanalysis models use observational data from the past to simulate climatology. The network of stations measuring radiation is sparse, therefore, reanalysis datasets are used as a representation of climatology. The accuracy of reanalysis radiation data can in part be explained by linking it to cloud amount in reanalysis. In this study, time-series analysis is performed to identify links between errors in radiation and cloud structures at different spatial scales, by making use of satellite imagery and reanalysis cloud data. This study examines two popular reanalysis datasets, MERRA2 from NASA and ERA-Interim from ECMWF, with the aim of establishing the skill of reanalyses when compared to ground measurements to find which is more suitable for solar radiation over Ireland. Reanalysis datasets are compared with a representative selection of Irish pyranometer data for time periods of up to 35 years, and standard skill scores (bias, RMSE and Pearson's correlation) are calculated. Scores relative to climate (Anomaly Correlation Coefficient (ACC)) are also calculated to compare the performance in different seasons.

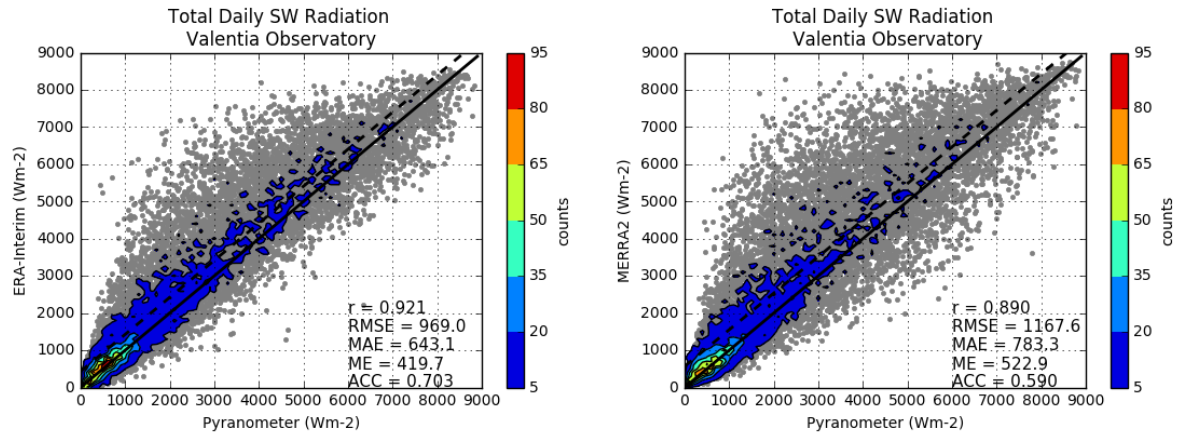

(a) ERA-Interim (b) MERRA2

Figure 7: Scatter density plot of pyranometer observations and ERA-Interim estimations (a) and MERRA2 estimations (b) at Valentia Observatory. Black solid line is the 1:1 line and black dashed line is the best fit line. Standard skill score results are printed in the bottom right.

Total daily shortwave radiation values were calculated at 7 station locations around Ireland with average pyranometer values of about $750 Wm^{-2}$ in winter and about $4500 Wm^{-2}$ in summer. Here, error is defined by subtracting pyranometer measurements from reanalysis model estimations, accordingly a positive error signifies the model radiation is greater than the observed radiation from the pyranometer. The standard skill scores suggest that ERA-Interim is a better overall representation of radiation than MERRA2. Skill scores calculated across stations show: bias is 479.74/ 299.54 Wm^{-2}, Pearson's correlation is 0.91/ 0.93, RMSE is 1062.1/ 876.63 Wm^{-2} and ACC is 0.614/ 0.717, for MERRA2 and ERA-Interim respectively.

Examination of individual pyranometers and the nearest grid point in the reanalysis model indicates that almost all locations perform better in ERA-Interim than MERRA2 (Valentia Observatory is shown as a representative station in figure 7), with the exception of RMSE at Dublin Airport which is slightly worse. Both ERA-Interim and MERRA2 reanalysis models overestimate total daily radiation compared to ground observations, similar to previous studies with different reanalysis datasets [2]. An ACC value of 60% corresponds to the range up to which there is synoptic skill for the largest scale weather patterns. An ACC value of 50% corresponds to forecasts for which the error is the same as for a forecast based on a climatological average. None of the stations in MERRA2 have an ACC score greater than 66%, whereas, 6 of the 7 ERA-Interim stations have ACC greater than 70%.

Other work [1] has found that the original MERRA reanalysis (before MERRA2) and ERA-Interim often simulate clear sky conditions when actual conditions are cloudy. The opposite was also true, although less pronounced: where actual clear sky conditions are simulated as cloudy. Variations in surface shortwave radiation occur primarily from interception by clouds between observation stations and the sun. In this study all stations show a larger absolute value for positive error events compared to negative error events, thus supporting this result.

The mean error was used to identify individual events with large errors in radiation. These events were analysed to find the prevailing cloud structure using both satellite imagery and the cloud data from reanalysis datasets. By linking cloud structure and errors in this way, initial analysis suggests that convective clouds are a source of negative bias in MERRA2 radiation, whereas frontal clouds are a source of positive bias. Knowledge gained from systematic errors in solar radiation in reanalysis models could be used to develop novel post processing techniques and produce an improved radiation dataset for Ireland.

References

[1] A. Boilley and L. Wald, Comparison between meteorological re-analyses from ERA-Interim and MERRA and measurements of daily solar irradiation at surface. *Renewable Energy* 75:135-143, 2015.

[2] X. Zhang, S. Liang, G. Wang, Y. Yao, B. Jiang and J. Cheng, Evaluation of the reanalysis surface incident shortwave radiation products from NCEP, ECMWF, GSFC, and JMA using satellite and surface observations. *Remote Sensing* 8(3):225, 2016.

The RKToolbox and Block Rational Arnoldi Method

Steven Elsworth[†], Stefan Güttel

School of Mathematics, Univeristy of Manchester
Alan Turing Building, Oxford Road, M13 9PL, Manchester, United Kingdom
[†]steven.elsworth@manchester.ac.uk

The rational Krylov Toolbox is a continuously developing collection of scientific computing tool based on rational Krylov techniques. The development started in 2013 and the current version contains, among other algorithms:

1. an implementation of Ruhe's (block) rational Krylov sequence method allowing the user to control various options, including non standard inner product, exploitation of complex-conjugate shifts, orthogonalisation, rerunning and parallelism [3];
2. methods for the implicit and explicit relocation of the poles of a rational Krylov space [2];
3. an implementation of RKFIT algorithm for rational least squares approximation [4];
4. the RKFUN class [4], allowing for numerical computations with rational functions.

Recent developments include the block rational Krylov sequence method [5] which has applications in solving linear systems with multiple right-hand sides, model order reduction [1], multiport RLC networks, and continuous-time algebraic Ricatti equations. The algorithm is a block generalisation of Ruhe's rational Arnoldi method but careful consideration must be taken to remove the possibility of a premature breakdown of the method due to linear dependencies of Krylov vectors. These dependencies can be avoided by using an appropriate choice of the so-called *block continuation vector*.

References

[1] O. Abidi, M. Hached, K. Jbilou, *Adaptive rational block Arnoldi methods for model reductions in large-scale MIMO dynamical systems*, New Trends Math. Sci., 4(2):227–239, 2016.

[2] M. Berljafa, S. Güttel, *Generalized rational Krylov decompositions with an application to rational approximation*, SIAM J. Matrix Anal. Appl., 36(2):894–916, 2015.

[3] M. Berljafa, S. Güttel, *Parallelization of the rational Arnoldi algorithm*, MIMS EPrint 2016.32 (http://eprints.ma.man.ac.uk/2503/), Manchester Institute for Mathematical Sciences, The University of Manchester, UK, 2016. Accepted for publication in SIAM J. Sci. Comput., 2017.

[4] M. Berljafa, S. Güttel, *The RKFIT algorithm for nonlinear rational approximation*, MIMS EPrint 2015.38 (http://eprints.ma.man.ac.uk/2530/), Manchester Institute for Mathematical Sciences, The University of Manchester, UK, 2015.

[5] S. Elsworth, S. Güttel, *The block rational Arnoldi method*, in preparation.

Error Correcting Codes using Unitary Units in Group Rings

Fergal Gallagher†, Leo Creedon

Institute of Technology Sligo, Ireland

†gallagher.fergal@itsligo.ie

This project involves the selection, analysis and construction of group rings and group ring elements which are suitable for the construction of high performing error correcting codes. Error correcting codes have applications within the communications area, such as mobile phones, PCs, digital radio, digital video, satellite and deep space communications. They enable communication between devices where the communication channel is subject to error due to noise, distance or power restrictions. Some of the best performing codes are self-dual. Group ring elements such as zero divisors and unitary units can be used to generate well known self-dual codes with powerful error correcting capability, using group ring matrices to form the generator matrix of a code. For example, Hurley and McLoughlin [3] used group ring matrices to construct the extended binary Golay (24,12,8) code. This is a self-dual code. This code was generated using the zero divisor $u = 1 + ab$ in F_2D_{24}, where $b = 1 + x + x^3 + x^4 + x^5 + x^6 + x^8$ is a unitary unit in F_2C_{12}, and the group D_{24} has the presentation $\langle x, a | x^{12} = a^2 = 1, x^a = x^{-1} \rangle$.

A generator matrix of an (n, k, d) code is a $(k \times n)$ matrix with rank equal to k whose rowspace is the set of all codewords. The minimum distance between the codewords is d. The distance between the codewords allows for the detection and correction of errors. For each group ring element we can form a group ring matrix and from this we can form a generator matrix. The aim of this project is to analyse the algebraic structure and properties of group rings and group ring elements that can generate efficient self-dual codes. Up to now, methods used to find suitable elements have used a computer search. A more favourable method is to refine the search by using algebraic methods.

Recent techniques by Broche and Del Rio [1] and the Perlis-Walker Theorem [4] are used to find the Wedderburn decomposition of group rings. These methods are used and adapted to give more general results for all possible semisimple group algebras for abelian groups. In doing this, we get a further insight into the isomorphism problem for group algebras. The Isomorphism problem concerns the following question:

Given two groups G and H and a field F, is it true that the existence of an isomorphism $FG \simeq FH$ implies that $G \simeq H$?

The answer to this question is no. In [2], Creedon gives the minimum counterexample to this problem. The non-isomorphic groups C_4 and C_2^2 have isomorphic group algebras over $\mathbb{F}_5$. That is, $\mathbb{F}_5(C_4) \simeq \mathbb{F}_5(C_2^2) \simeq \bigoplus_{i=1}^{4} F_5$.

Here we show that this is a specific example of a general class.

Given two non-isomorphic abelian groups G and H each with order n, and a field F of order q such that $q \equiv 1 (mod\ n)$, then

$$FG \simeq FH \simeq \bigoplus_{i=1}^{n} F_q$$

Another example of this is $\mathbb{F}_{3^2}(C_4 \times C_2) \simeq \mathbb{F}_{3^2}(C_8) \simeq \bigoplus_{i=1}^{8} F_{3^2}$.

We show that there is another class of isomorphic group algebras.

Given two non-isomorphic abelian groups G and H each with order n and each containing exactly m elements of order dividing 2, and a field F of order q such that $q \equiv$ -1$(mod\ e)$ where e is the exponent of the group, then $FG \simeq FH$. In this case,

$$FG \simeq FH \simeq \bigoplus_{i=1}^{m} F_q \oplus \bigoplus_{i=1}^{[n-(m)]/2} F_{q^2}$$

For example $\mathbb{F}_7(C_2 \times C_4 \times C_8) \simeq \mathbb{F}_7(C_4^3) \simeq \bigoplus_{i=1}^{8} F_7 \oplus \bigoplus_{i=1}^{28} F_{7^2}$.

We also show that the minimal isomorphic pair of group algebras FG and FH (with G and H not isomorphic) which is not of either of the two types above is $\mathbb{F}_5 C_{12}$ and $\mathbb{F}_5(C_2 \times C_6)$. For the first group algebra, $|F| \equiv 5(mod\ 12)$. Here $\mathbb{F}_5 C_{12} \simeq \mathbb{F}_5(C_2 \times C_6) \simeq \bigoplus_{i=1}^{4} F_5 \oplus \bigoplus_{i=1}^{4} F_{5^2}$.

Acknowledgement. The research has received funding from the IT Sligo President's Bursary Award.

References

[1] O. Broche and A. del Rio, *Wedderburn decomposition of finite group algebras.* Finite fields and Their Applications (2007), 71-79.

[2] L. Creedon, *The Unit Group of Small Group Algebras and the Minimum Counterexample to the Isomorphism Problem*, International Journal of Pure and Applied Mathematics, Volume 49 No. 4 (2008), 531-537.

[3] Hurley T and McLoughlin I, *A Group Ring Construction of the Extended Binary Golay Code*, IEEE Trans. Inf. Theory, September 2008, vol. 54, no. 9, pp. 4381-4383.

[4] C. Polcino Milies and S. K. Sehgal, *An Introduction to Group Rings.* Kluwer Academic Publishers (2002).

Comparison of Correlations Between Wind and Solar Radiation Across Multiple Datasets

Seanie Griffin[†1,2], Conor Sweeney[1,2]

[1]UCD Energy Institute, University College Dublin, Dublin, Ireland
[2]School of Mathematics and Statistics, University College Dublin, Dublin, Ireland

[†]seanie.griffin@ucdconnect.ie

Combined wind and solar (PV) power generation has potential to offer a stable supply of energy. This is done to lessen the problem of intermittency by making use of any possible negative correlation between wind speed and solar radiation. Preliminary site assessment for a combination of wind and solar power generation is commonly done by making use of reanalysis data. A comparison of the variability between wind speed and solar radiation in reanalysis was examined in [1] for the UK, finding a negative correlation between them. The amount of solar radiation reaching the surface is greatly influenced by cloud cover, especially in reanalysis [2]. The impact that cloud cover can also have on wind speeds was investigated in [3]. It was found that the presence/absence of cloud cover can produce varied distributions of wind speed at different heights near the surface. In this study, two popular reanalysis datasets, ERA-Interim and MERRA2, have been compared to wind and pyranometer data from synoptic stations at representative locations around Ireland. Correlation between wind and shortwave radiation for reanalysis data is being compared to the correlations from observational data.

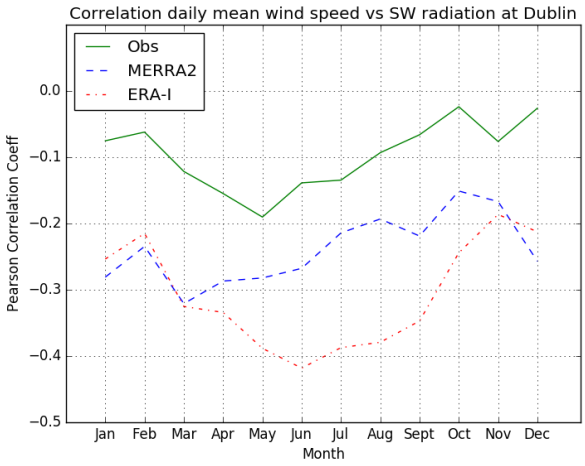

Figure 8: Monthly correlations of daily mean 10m wind speed and shortwave radiation at Dublin Airport for observations (green, solid), MERRA2 (blue, dashed) and ERA-Interim (red, dash-dot).

Observations from four Irish synoptic stations, which have colocated 10m wind speed and pyranometer measurements, are used. Analysis of the Pearson correlation coefficients between daily mean 10m wind speed and incoming shortwave radiation has found differences between each of the datasets. As an example fig.8 shows the correlations, broken down by month, at Dublin Airport. Both reanalyses have overestimated the strenth of the relationship between wind speed and solar radiation at Dublin Airport. The relatively coarse resolutions of the reanalyses (50km and 78km for MERRA2 and ERA-Interim respectively) means that both datasets will struggle to capture small scale boundary layer processes which may be causing these differences. As a result, reanalysis wind speeds which are further away from the surface will also be considered.

The complementary relationship between wind and solar was examined in [1] for the UK. Using ERA-Interim data, it was found that the magnitude of the negative correlation between wind speed at 60m and solar radiation was greatest during the summer months. These calculations are repeated here for Ireland using both reanalyses. The wind speeds used were at heights of 50m and 60m for MERRA2 and ERA-Interim respectively. These are averaged spatially and temporally to produce a series of daily mean wind speed and shortwave radiation values for Ireland as a whole. The correlations between wind speed and radiation for each month are shown in fig.9. For ERA-Interim, fig.9a, the largest negative correlation occurs during the summer; though it is less pronounced than in [1]. Meanwhile for MERRA2, fig.9b, the magnitude of the correlation coefficient is larger during the winter.

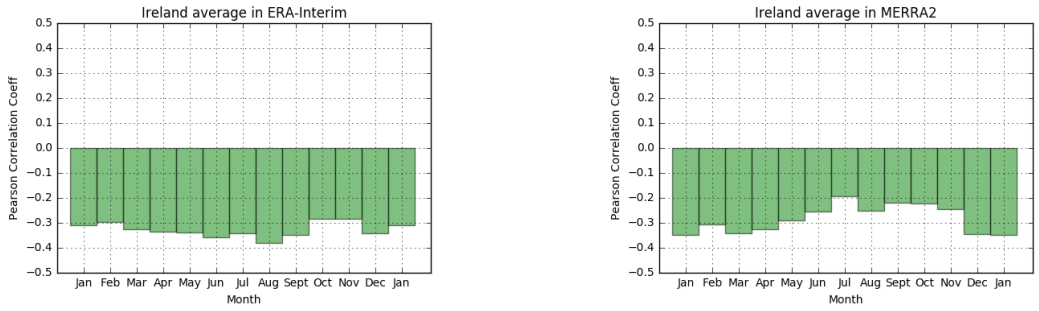

(a) ERA-Interim (b) MERRA2

Figure 9: Monthly correlations of daily mean wind speeds with solar radiation for (a) ERA-Interim and (b) MERRA2. (Wind speeds at heights of 50m and 60m respectively).

Future work will be performed using mast observations of wind speed away from the Earth's surface to assess the performance of each reanalysis at producing a realistic relationship between wind speed and solar radiation over Ireland.

References

[1] P. E. Bett and H. E. Thornton, The climatological relationships between wind and solar energy supply in Britain. *Renewable Energy* 87:96-110, 2016.

[2] A. Boilley and L. Wald. Comparison between meteorological re-analyses from ERA-Interim and MERRA and measurements of daily solar irradiation at surface. *Renewable Energy* 75:135-143, 2015.

[3] Y. He, A. H. Monahan and N.A. McFarlane. Diurnal variations of land surface wind speed probability distributions under clearsky and lowcloud conditions. *Geophysical Research Letters* 40(12):3308-3314, 2013.

Derivation Codes

Kieran Hughes[†], Leo Creedon

Institute of Technology Sligo, Ireland

[†]kieran.hughes@mail.itsligo.ie

Error correcting codes play an essential role in the effective transmission of data. Applications include satellite communication, data compression and storage, networking, synchronisation and cryptography. The basic parameters of a code are field size, length, dimension and minimum distance. The problem is to optimise these conflicting parameters so as to form a bespoke code that has the right parameters for a particular task. The solution proposed here is to apply derivations (linear transformations satisfying Leibniz's rule for multiplication) to group algebras. The image of the group algebra under a derivation (and all of its iterations) gives a subspace. This gives a method for constructing codes (subspaces). The task is to analyse the parameters of these codes using the structure of the derivations and the underlying group algebras. It may then be possible to choose the group algebra and the derivation such that a particular combination (direct sum) of subspaces leads to a code with the desired parameters.

A derivation on a ring R is an additive group homomorphism that satisfies a multiplicative rule known as Leibniz's rule. Thus d is a derivation on a ring R, if it satisfies the following two equations, for all elements x and y in the ring R

$$d(x+y) = d(x) + d(y) \tag{18}$$

$$d(xy) = d(x)y + xd(y). \tag{19}$$

The set of all derivations on a group algebra KG has the structure of a ker_d-module, where ker_d is the kernel of the derivation d.

Lemma. Let R be a unital ring with characteristic p and C_{p^n} the cyclic group generated by the element x. Then there exists a unique derivation d on the group ring C_{p^n} such that

$$d(x) = 1 \quad and \quad d(R) = 0. \tag{20}$$

Lemma. Let $G = H \times A$ be a finite abelian group, where H is a p regular group and A is a p group with a minimum number of generators t. Then

$$|Der(\mathbb{F}_{p^n}G)| = |\mathbb{F}_{p^n}G|^t = p^{n|G|t} \tag{21}$$

A group algebra is a vector space V over a field K. A derivation can be represented by a linear transformation $T\colon V \to V$. The image of the group algebra under the linear transformation T is a T-invariant subspace W of V. Denote the restriction of T to W by $T\restriction_W$. Then $T\restriction_W\colon W \to W$ is a linear transformation and the image of W under $T\restriction_W$ is a $T\restriction_W$-invariant subspace of W. In this way the process can be continued. However, there exists an integer m such that after m steps the derivation map is an isomorphism on the range space of the transformation T^m.

Linear block codes are subspaces of a vector space. The q-ary $[n, k, \delta]$ code is a linear code of length n, dimension k and minimum distance δ. We can form codes by applying a derivation to a group algebra. The resulting subspaces are linear codes.

Example: Let $KG = \mathbb{F}_2 C_8$ and let d be the derivation defined on KG by

$$d\colon \mathbb{F}_2 C_8 \to \mathbb{F}_2 C_8 \quad where \quad x \mapsto x^2 + x^4 + x^6 + x^7 \tag{22}$$

The range space of this derivation is a 4-dimensional subspace of $\mathbb{F}_2 C_8$. This subspace is an $[8, 4, 4]$ binary code. In fact, it is equivalent to the extended binary Hamming code Hâm$(3, 2)$. It can simultaneously correct any single error and detect any double error.

The objective is to establish a relationship between the derivation on a group algebra and the code and to exploit this relationship to design codes with certain properties.

Acknowledgement. The research has received funding from the Institute of Technology Sligo Presidents Bursary Award.

Inline Product Characterization of Polylactide (PLA) during Melt Extrusion Processing using the Random Forest Algorithm

Konrad Mulrennan[†1], Marion McAfee[1], John Donovan[1], Leo Creedon[1], Fraser Buchanan[2] and Mark Billham[2]

[1]Department of Mechanical and Electronic Engineering, Institute of Technology Sligo
[2]School of Mechanical and Aerospace Engineering, Queen's University Belfast

[†]mulrennan.konrad@itsligo.ie

Polylactide (PLA) is a biodegradable polymer with numerous applications across the biomedical, pharmaceutical and packaging industries. In the medical device industry PLA is used to create implants such as fixation screws, tissue scaffolds and sutures. These devices offer support and ideally degrade at the same rate as the body heals which eliminates the need for a second operation. The melt processing of PLA faces challenges due to its poor thermal stability which is influenced by processing temperatures and shearing. Finding optimised melt processing conditions is generally based on trial and error and is very sensitive to batch to batch variations. The characterization of processed products takes place offline in laboratory environments. This can result in the manufacturer completing full production runs while having no knowledge on whether the product is in or out of specification. As a result, typical scrap rates of a PLA medical grade product can be up to 25-30%. This work discusses the development of Random Forest mathematical models for a twin screw melt extrusion process. The resulting models can predict product end characteristics from inline data. These include mechanical properties and percentage mass change of a product during its degradation cycle. These models can provide real time feedback on the changes to product end characteristics during melt processing. This will reduce manufacturing costs and minimize waste as well as accurately predicting future performance and behaviour of products.

Random forests provide a great opportunity in the monitoring and control of polymer extrusion processing. The model discovers lower and higher order interactions as well as nonlinearity between predictor variables (i.e. system measurements such as pressure, temperature or torque) and responses (i.e. what is desired to be predicted) without having to give the model any prior information. The random forest tends to have a low generalization error (the error expected on new data) and is usually much less computationally expensive than other machine learning algorithms. The random forest has excellent performance using the default tuning parameters and requires no preprocessing of the data.

The random forest models were built by aggregating a number of bootstrapped decision trees. The decision trees are logic rules based models made up of if-then-else statements which select the predictor variable and split value which best partitions the data to minimise the residual sum of squares in each of the subsets. Each decision tree has a low bias as the model looks to minimise the error at each split. Bootstrap data sets are generated for each decision tree in the Random Forest. Each bootstrap data set is a random sample of the original data taken with replacement and is the same size as the original data set. A bootstrap data set contains ≈63% of the original data set. The predictions from the bootstrapped decision trees are then aggregated to get the overall prediction of the Random Forest model. The bootstrap aggregation modelling approach has had the term "Bagging" coined for it. The ≈37% of data from the original data set which is not used to create each bootstrap data set is used to create an Out-Of-Bag (OOB) error estimation which removes the need for cross-validation and requires little additional computing. The introduction of a tuning parameter m (m is commonly referred to as m_{try} in the literature) allows the Random Forest model to control the number of predictor variables to choose from to split the data at any node. This means that at each split point in a tree, a random subset of all available predictors is created. The use of this tuning parameter results in a variance reduction in the models.

The random forest models have demonstrated accurate prediction of the maximum force at break of samples at various time points including before and during the product's degradation cycle. Further to this the models have also accurately predicted the percentage mass change of the extruded sheet at each of the time points during the samples' degradation cycle. The mathematical models described in this work can be implemented with minimal change to existing extrusion lines. By only using inline pressure measurements from a slit die and shear viscosity estimates from a twin screw melt extrusion process for PLA, models have been developed which have successfully predicted the end material characteristics of the extruded sheet at each of the time points during the samples' degradation cycle. The success of the models could enable the development of a system that can alert system operators to processing issues in real time rather than having to wait for the offline laboratory analysis. By implementing these mathematical models as soft sensors in a production line, a manufacturer could save time and raw material if the models indicated that the products are going out of specification.

Acknowledgement

- The research leading to these results has received funding from the European Union's Seventh Framework Programme managed by REA-Research Executive Agency http://ec.europa.eu/research/rea (FP7/2007-2013) under grant agreement n°605086FP7-SME-2012
- The research leading to these results has received funding from the Institute of Technology Sligo Presidents Bursary Award 2012
- The research leading to these results has received funding from the Institute of Technology Sligo Research Capacity Building Fund 2016/17

Evaluating Password Advice

Hazel Murray[†1], David Malone[2]

[1]Department of Mathematics and Statistics
Maynooth University, Maynooth, Co. Kildare, Ireland
[2]Hamilton Institute
Maynooth University, Maynooth, Co. Kildare, Ireland

[†]hazelmsmurray@gmail.com

Abstract

Password advice is constantly circulated by standards agencies, companies, websites and specialists. Yet there appears to be great diversity in the advice that is given. We collected password advice and found that the advice distributed by one organization can directly contradict advice given by another. By categorizing the advice, we gained insight into the composition of advice circulated to users and organization and were able to identify key costs associated with the implementation of this advice.

Background

Herley [1] argues that users' rejection of security advice is rational from an economic perspective. Indeed, Inglesant and Sasse [2] find that users are concerned with maintaining security, but that existing security policies are too inflexible to match their demands. We conduct a systematic study to identify characteristics and analyse costs.

Collecting and Categorizing Advice

We collected 269 pieces of password advice from 21 different sources.

To extract meaning we divided the advice into categories. For this we considered each piece of advice individually. The first pieces of advice we examined suggested our starting categories. From there, each piece of advice was either included in one of our existing categories, expanded the scope of an existing category or created a new category to suit it. In total, we identified 29 advice categories.

Once we divided the advice into categories we noticed the pieces of advice within each category did not necessarily promulgate similar opinions. It was therefore necessary to subdivide the advice into statements which offer a similar message.

The adjacent figure shows the statements associated with a subset of the identified categories. Also shown are the number of sources who support or are against the given advice statement.

	#A	#S
Phrases		
Don't use patterns.	0	6
Take initials of a phrase.	0	4
Don't use published phrases.	1	2
Substitute symbols for letters.	1	2
Don't use words.	0	16
Composition		
Must include special characters	5	7
Don't repeat characters.	0	3
Enforce restrictions on characters.	1	12
Expiry		
Store history to eliminate reuse.	0	5
Have a minimum Password Age.	0	1
Change your password regularly.	4	7
Change if suspect compromise.	0	10
Personal Information		
Don't include personal information.	1	5
Must not match account details.	0	8
Do not include names.	1	8
Personal password storage		
Don't leave in plain sight.	0	4
Don't store in a computer file.	1	2
Write down safely.	1	6
Don't choose "remember me".	0	3

#A = number against the advice.
#S = number supporting advice.

Identification of Cost Categories

For each advice statement we identified costs that could be associated with their enforcement. After analyzing each of the 78 statements we had defined 10 categories of costs that we believe provide a rudimentary understanding of the general costs associated with obeying password advice. These are shown in the above table.

1.	Increased risk of forgetting.
2.	Need to pick a new password.
3.	Possible multiple attempts needed to enter a valid password.
4.	Inconveniences use of a personal system for password generation.
5.	User time taken.
6.	Reduced entropy.
7.	Organizations' time taken to enforce/program.
8.	Impossible/hard to enforce.
9.	Creates an additional security hole.
10.	Increased computing power needed.

Quantifying Costs

We now want to create parameters for each of the cost categories. This will allow us to quantify the costs associated with enforcing password advice.

For example, we have graphical results to depict the change in entropy of a password set resulting from the introduction of composition restrictions.

$$Entropy = -\sum_{i=1,n} p_i . \log_2 (p_i) \qquad Guesswork = \sum_{i=1,n} i.q_i \tag{23}$$

where p_i and q_i are sequences of probabilities and q_i is a nonincreasing sequence with q_1 the most likely.

Summary

Our collection and categorization of advice and identification of cost categories brought discrepancies in password advice into focus. Contradictory information and the burden of costs on the user may reflect one of the reasons for users' unwillingness to follow advice. We are now in the process of quantifying each of the costs identified. This will provide a better understanding of the costs versus benefits of password advice.

Acknowledgements. This publication has emanated from research supported in part by a research grant from Science Foundation Ireland (SFI) and is co-funded under the European Regional Development Fund under Grant Number 13/RC/2077. This research is also supported by a John and Pat Hume doctoral studentship.

References

[1] Cormac Herley. So long, and no thanks for the externalities: the rational rejection of security advice by users. In *Proceedings of the 2009 workshop on New security paradigms workshop*, pages 133–144. ACM, 2009.

[2] Philip G Inglesant and M Angela Sasse. The true cost of unusable password policies: password use in the wild. In *Proceedings of the SIGCHI Conference on Human Factors in Computing Systems*, pages 383-392. ACM, 2010.

Theory of Coupled Lasers

Christopher Patrick O Connor†, Sebastian Wieczorek, Andreas Amann

Department of Applied Mathematics, School of Mathematical Sciences, University College Cork

†christopherconnor@umail.ucc.ie

Coupled Laser Theory is an area yet to be fully understood. Since the first lasers of the 1960s, we have seen huge developments in the field. An important step which paved the way for coupled lasers was Semiclassical Laser Theory [1]. Lamb introduced this theory in the early 1960s which used both parts of Quantum Mechanics and also Maxwell's Equations to create a suitable description of a single atom laser where the cavity was closed by solving,

$$\nabla \times \nabla \times \vec{E} + \mu_0 \sigma \frac{\partial \vec{E}}{\partial t} + \mu_0 \epsilon_0 \frac{\partial^2 \vec{E}}{\partial t^2} = -\mu_0 \frac{\partial^2 \vec{P}}{\partial t^2}, \tag{24}$$

where $\vec{E}$ is the electric field, $\vec{P}$ is the polarisation and σ is the fictional conductivity. From there, research extended into a coupled laser system ([2],[3]) using the semiclassical approach while dealing with a closed system once again.

From the theories mentioned above, they used atom lasers and gas lasers which were the first types to be invented. However research has moved to focus on semi-conductor lasers as they are more compact and are less expensive with more applications. Furthermore, previous theories deal with closed systems which today are relatively known. Our research deals the coupling of laser cavities in an open system, an area which is not fully understood and is important in the area of Photonics.

To achieve this, we need to create a suitable mathematical model which can effectively describe the physics behind what occurs. From there, we can use techniques from Nonlinear Dynamics to provide a stability analysis of the coupled laser system. To begin, our current focus lies in Coupled Mode Theory [4] which we aim to describe what occurs in a linear coupled system with losses. The equations for this are,

$$\dot{a_1} = (i\omega_1 - \gamma_1)a_1 + i\kappa a_2 \tag{25}$$

$$\dot{a_2} = (i\omega_2 - \gamma_2)a_2 + i\kappa a_1 \tag{26}$$

where ω_i is the frequency, γ_i the losses, κ is the coupling constant. Unlike some researchers, we do not assume the coupling constant to be purely real and have actually shown, that complex coupling is allowed with certain restrictions.

References

[1] Lamb Jr, Willis E. "Theory of an optical maser." *Physical Review* 134.6A (1964): A1429.

[2] Spencer, Martin B., and Willis E. Lamb Jr. "Theory of two coupled lasers." *Physical Review A* 5.2 (1972): 893.

[3] Shakir, Sami A., and Weng W. Chow. "Semiclassical theory of coupled lasers." *Optics letters* 9.6 (1984): 202-204.

[4] Haus, Hermann A., and Weiping Huang. "Coupled-mode theory." *Proceedings of the IEEE* 79.10 (1991): 1505-1518.

Risk profiles and their association with the development of new pain in older Irish adults: a latent class analysis

Aoife O'Neill†, Cathal Walsh and Helen Purtill

Department of Mathematics and Statistics, University of Limerick, Ireland
†aoife.oneill@ul.ie

Abstract: The aim of this study is to examine whether risk profiles of physical health, mental health and lifestyle behaviour factors can predict the development of new pain, in older Irish adults. Latent class analysis (LCA) was used to identify different risk profiles in a sample of people aged over 50, from The Irish Longitudinal Study on Aging (TILDA), who reported being pain-free at Wave 1 and participated in the follow-up interviews two years later, at Wave 2, (N=4,349). Four latent classes were identified based on 11 health risk factors from Wave 1. Associations between the profiles and new pain development after two years were examined.

Introduction

In 2016 the Organisation for Economic Cooperation and Development (OECD) reported that Ireland had one of the fastest growing life expectancy rates in Europe [3]. Pain can be considered a significant restriction to the quality of life and well-being of older adults. Past research has shown links between pain and a number of multidimensional factors, such as sleep problems [2], poorer general health [4] and depression [1]. Thus, with our aging population it is important to examine the association between risk profiles and the development of new pain.

Methods

The TILDA study is a nationally representative cohort study of adults, aged 50 years and older, living in the Republic of Ireland. For this analysis it was of interest to examine health risk factors for a sample of individuals who did not suffer from pain at Wave 1 and who participated in follow-up interviews at wave 2 (N=4,458).

LCA was used to identify health risk groups based on 11 physical health, mental health and lifestyle behaviours. LCA provides a probability model-based approach to measuring categorical variables with the aim of identifying underlying subgroups in a population based on some measured characteristics. The optimal number of latent classes was based on a number of model-fit indices. The association between class membership and future pain development was examined using a classify-analyse approach, where individuals were assigned to a latent class using their Posterior Probabilities and logistic methods were used to predict new pain.

Results

Using LCA, four latent classes were identified. These health risk classes were characterised as Low Risk, Physical Health Risk, Mental Health Risk and High Risk. The Low Risk class accounted for over half the sample (51.1%), while the High Risk class accounted for 7.8% of the sample. At follow-up (Wave 2), 797 (17.87%) of the participants reported new pain development. Those in the High Risk class were at an increase risk of developing pain two years later (OR=3.63, 95% CI = 2.78, 4.73) when compared to those in the Low Risk class.

Conclusion

LCA analysis identified four health risk profiles for pain-free older Irish adults, based on their mental and physical health and lifestyle behaviours. These latent classes were predictive of new pain development in older people.

References

[1] Lin EH, Katon W, et al. (2003). Effect of improving depression care on pain and functional outcomes among older adults with arthritis: a randomized controlled trial. *Jama*, pp. 290(18):2428-9.

[2] Lus Blay S, Andreoli SB, Leite Gastal F (2007). Chronic painful physical conditions, disturbed sleep and psychiatric morbidity: results from an elderly survey *Annals of Clinical Psychiatry*, 19(3):169-74.

[3] OECD (2016). Health at a Glance: Europe 2016. *OECD Publishing*.

[4] Mntyselk PT, Turunen JH, et al. (2003). Chronic pain and poor self-rated health. *Jama*, 290(18):2435-42.

Time Series Modelling and Forecasting of Hospital Overcrowding in Ireland

Jean Abi Rizk[†], Cathal Walsh

MACSI, Department of Mathematics and Statistics, University of Limerick, Limerick, Ireland

[†]Jean.Rizk@ul.ie

Abstract: According to the daily trolley count by the Irish Nurses and Midwives Organisation (INMO), the overcrowding crisis in Irish hospitals has reached a new record at the start of 2017 with more than 600 patients on trolleys. This work presents a time series approach to model the INMO data and to present future predictions of the overcrowding in Irish hospitals. The structure of the data exhibits short and long seasonal patterns, a moving peak occurring at the start of every year and a significant trough that occurs conditionally after the peak. While seasonal ARIMA models fail to capture multiple seasonality with long seasonal periods [1], we present a time series modelling approach that is a combination of a Fourier series to model the long seasonal pattern and a seasonal ARIMA process to model the short-term dynamics. The moving peak and the trough are modelled with regression-type models [2]. The model shows reasonable forecasts that approximately match the actual 2017 data showing that the high records of 2017 could have been predicted in advance.

Introduction

The data is a daily record from 2013 to 2016 of the number of patients waiting on trolleys. The decomposition of the time series revealed a weekly (short period) and yearly (long period) seasonality. Seasonal versions of ARIMA models are designed for short periods. Fitting an ARIMA model with a period > 200 requires long computational times and excessive amount of memory. We use a Fourier series approach to model the long seasonal pattern. The weekly seasonality along with the trend and the random components are all modelled by an ARIMA process.

Methodology

The data obtained from the INMO were missing the weekends. We therefore, considered the week to be of 5 days and the year of 261 days. The hospitals are divided into two categories, Countryside and Eastern. The two time series were decomposed into trend, seasonal and random components. The decomposition as well as the autocorrelation function revealed a weekly and a yearly seasonality with periods 5 and 261 respectively. The series may be modelled as follows:

$$Y_t = \alpha + \sum_{k=1}^{K} [a_k cos(2\pi t/p) + b_k sin(2\pi t/p)] + X_t + R_t, \tag{27}$$

where Y_t is the series under investigation, X_t is a seasonal ARIMA process and R_t are regressors. $p = 261$ is the long seasonal period and the value of K can be chosen to minimise the AIC. The forecasts along with the trends are shown in Fig.1.

Conclusion

The forecasts captured the high numbers that were already recorded by the INMO early this year. The data also showed that the Countryside Hospitals exhibit an increasing trend but the trend of the Eastern data showed multiple overcrowding phases (Fig.1). This data will be a proxy for modelling the arrival

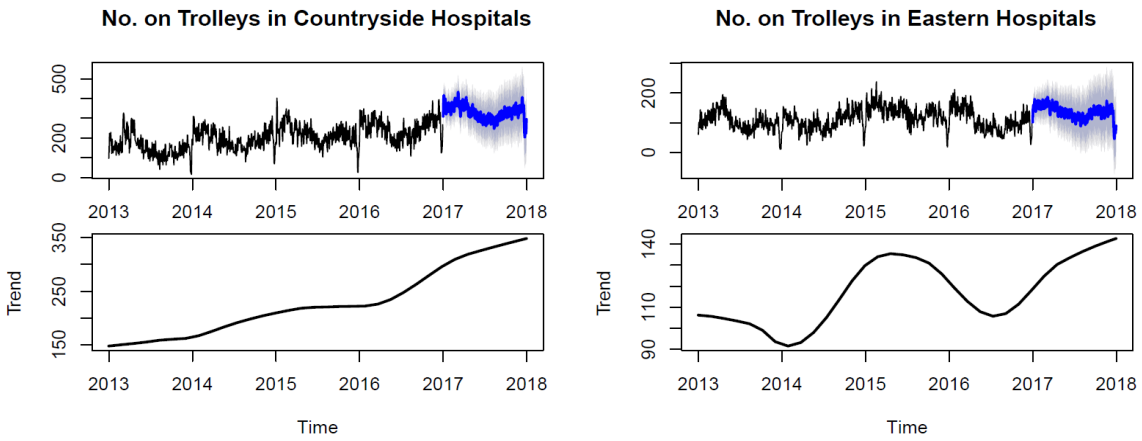

Figure 10: Forecasts and trends of Countryside and Eastern Hospitals' data

rate of patients into the hospital that will be used in our time-dependent queueing model which will be presented in future work.

References

[1] A.M. De Livera, R.J. Hyndman and R.D. Snyder, Forecasting time series with complex seasonal patterns using exponential smoothing. *Journal of the American Statistical Association*, 106,1513 – 1527, 2011.

[2] W. R. Bell, and S. C. Hillmer, Modelling time series with calendar variation. *Journal of the American statistical Association* 78.383, pp. 526 – 534, 1983.

Mathematical Modelling of Bovine Follicular Dynamics

Malgorzata Wieteska[†1], Leo Creedon[1], John A Hession[1], Stephen T Butler[2]

[1]Institute of Technology Sligo, Ireland [2]Teagasc

[†]Malgorzata.Wieteska@mail.itsligo.ie

Abstract

In the beef and dairy industries, predicting the number of follicular waves emerging, the time of ovulation and the presence of multiple ovulation is an important problem where infertility is increasingly prevalent and where twinning has a major financial impact. To better understand these issues, mathematical models of bovine follicles are developed and fitted to experimental data. These models include (1) systems of differential equations modelling hormonal interactions, (2) a geometric model of the follicle which estimates the volume of cells producing different hormones and (3) a Markov process using probability transition matrices to predict follicular development.

Hormonal interactions during the estrus cycle

The follicular dynamic is controlled by feedback mechanisms. Two main structures on the ovary producing hormones are the follicle and the corpus luteum. The granulosa cells of follicles produce estradiol and inhibin, which in turn controls the release of FSH (follicle stimulating hormone) needed for growth of the follicles $< 8mm$. Thereafter, follicle(s) need LH (luteinizing hormone) in order to grow. The CL (corpus luteum) produces progesterone, which is decreased after the surge of the prostaglandin. This causes the regression of the CL. The release of FSH and LH is regulated by GnRH (gonadotropin-releasing hormone) [4].The LH synthesis and release is affected also by estradiol [1]. The LH surge causes ovulation and as an effect there is no production of estradiol and inhibin [4]. The release of GnRH is governed by progesterone, having a negative feedback and estradiol having a positive effect during pro-estrus and negative during the luteal phase of the estrus cycle [1]. A surge of GnRH is released when oestradiol reaches a critical level, which occurs when dominant follicle reaches a threshold size [4].
IGF-1 enhances production of estradiol by granulosa cells (by affecting an activity of the aromatase activity) of the follicle as well as increases the granulosa cells number. However, after exceeding certain level IGF-1 inhibits its stimulation of estradiol production, FSH works in a similar way to IGF-1 [3]. IGF-1 is produced in small quantities by follicles and is mainly produced by the liver, and delivered with blood to the follicle. The system of differential equations (which is validated at present) incorporates an effect of IGF- 1 on the estrus cycle.

Model of follicle geometry

Hypothesis: As the follicle grows, there is a mathematical relationship between the diameter of the antrum and the thickness of the cellular layers (granulosa and theca). This relationship continues even after the thickness of granulosa layer becomes constant. In order to be able to create a geometric model of the follicle, the histology of follicles was performed. Cross-sections were analysed under a microscope and measurements were taken and used to create the model. The follicle is composed of the antrum (cavity filled with the follicular fluid), encompassed by the granulosa cell layer and the theca layer, both of which are part of the follicle wall. This model was used to create the model of volume of granulosa depending on the diameter of the follicle.

Probability transition matrix

Follicular dynamics can be treated as an example of a Markov chain, with the simplifying assumption that future states of the follicle depend only on the present state. Therefore the transition probability matrix P is used. The calculated probabilities of staying in the given states or transfer to another state on the following day were calculated. Each row of the matrix shows the probability of follicles of the corresponding state being transferred into another state (matrix columns), or staying in the same state. The probabilities in each row must add up to 1. The following states were assumed: ReF (follicles between $5-6mm$), SeF (follicles between $6-8mm$), DmF (follicles $> 8mm$), CL1 (growing corpus luteum), CL2 (corpus luteum in the static phase of growth), CL3 (degenerating corpus luteum), Atr (denoted atretic follicles), N (Nothing, denoted that the follicle or corpus luteum has 'died'). The probabilities were calculated for each cow starting 1 day before estrus and continue for the length of the estrus cycle for the respective cow. The probability transition matrix P for a cow with an estrus cycle with three follicular waves is shown. This matrix P can be used to calculate the probabilities in the required time interval (using P^N , where N stands for the length of the time interval). For example this would permit an animal breeder taking an ultrasound scan to predict the likely state of a dominant follicle several days into the future.

Acknowledgement. The research has received funding from the Institute of Technology Sligo President's Bursary Award.

References

[1] *Boer, H.M.T., Stötzel, C., Röblitz, S., Deuflhard, P., Veerkamp, R.F. and Woelders, H.,* A simple mathematical model of the bovine estrous cycle: follicle development and endocrine interactions. *Journal of theoretical biology* 278(1), pp.20-31, 2011.

[2] *Grinstead, C.M. and Snell, J.L.* Introduction to probability. *American Mathematical Soc..*, 2012.

[3] *Gutierrez, C.G., Campbell, B.K. and Webb, R.* Development of a long-term bovine granulosa cell culture system: induction and maintenance of estradiol production, response to follicle-stimulating hormone, and morphological characteristics. *Biology of reproduction*, 56(3), pp.608-616, 1997.

[4] *Pring, S.R., Owen, M., King, J.R., Sinclair, K.D., Webb, R., Flint, A.P. and Garnsworthy, P.C.,* A mathematical model of the bovine oestrous cycle: Simulating outcomes of dietary and pharmacological interventions.*Journal of theoretical biology* 313, pp.115-126, 2012.

List of Participants

Jean	Abi Rizk	University of Limerick	Jean.Rizk@ul.ie
Daher	Al Baydli	NUI Galway	daher.mathematics@gmail.com
Nisreen	Alokbi	NUI Galway	nisreen.alokbi@gmail.com
Faiza	Alssaedi	NUI Galway	f.alssaedi1@nuigalway.ie
Jehan	Alswaihli	University of Reading	jehanalswaihli@gmail.com
Kholoud	Alzubaidi	Maynooth University	kholoud.alzubaidi.2017@mumail.ie
Maram	Arishi	Maynooth University	maramareshi@gmail.com
Kevin	Brosnan	University of Limerick	kevin.c.brosnan@ul.ie
Richard	Burke	NUI Galway	richardburke8@gmail.com
Sinead	Burke	University of Limerick	sinead.burke@ul.ie
Hannah	Conroy Broderick	NUI Galway	h.conroybroderick1@nuigalway.ie
Francisco	de Melo Virissimo	University of Bath	fdmv20@bath.ac.uk
Léa	Deleris	IBM Dublin Research Lab	lea.deleris@ie.ibm.com
Michel	Destrade	NUI Galway	michel.destrade@nuigalway.ie
Eadaoin	Doddy	University College Dublin	eadaoin.doddy@ucdconnect.ie
Edward	Donlon	Dublin Institute of Technology	edward.donlon1@mydit.ie
Joshua	Duley	University of Limerick	joshua.duley@ul.ie
Steven	Elsworth	The University of Manchester	steven.elsworth@manchester.ac.uk
James	Fannon	University of Limerick	james.fannon@ul.ie
Patrick	Farrell	University of Oxford	patrick.farrell@maths.ox.ac.uk
Roberto	Galizia	NUI Galway	r.galizia1@nuigalway.ie
Fergal	Gallagher	IT Sligo	gallagher.fergal@itsligo.ie
Craig	Gilmour	University of Strathclyde	craig.gilmour@strath.ac.uk
Paul	Greaney	NUI Galway	paul.greaney@nuigalway.ie
Sean	Griffin	University College Dublin	seanie.griffin@ucdconnect.ie
Danny	Groves	Cardiff University	grovesd2@cardiff.ac.uk
Aoife	Hill	NUI Galway	aoife.hill03@gmail.com
Róisín	Hill	NUI Galway	r.hill2@nuigalway.ie
Sally	Hill	Cardiff University	hillsl2@cardiff.ac.uk
Kieran	Hughes	IT Sligo	kieran.hughes@mail.itsligo.ie
Garrett	Jordan	GMIT	garrett.jordan@research.gmit.ie
Alex	Mackay	Cardiff University	mackaya1@cardiff.ac.uk
Niall	Madden	NUI Galway	niall.madden@nuigalway.ie
Vinh	Mai	NUI Galway	q.mai1@nuigalway.ie
Robert	Mangan	NUI Galway	r.mangan4@nuigalway.ie
Christine	Marshall	NUI Galway	c.marshall1@nuigalway.ie
Aisling	McGlinchey	Maynooth University	mcglinchey1209@gmail.com
Niall	McInerney	University of Limerick	mackard57@gmail.com
Martin	Meere	NUI Galway	martin.meere@nuigalway.ie
Scott	Morgan	Cardiff University	MorganSN@cardiff.ac.uk
Konrad	Mulrennan	IT Sligo	mulrennan.konrad@itsligo.ie
Hazel	Murray	Maynooth University	hazmurray93@gmail.com
Christopher	O Connor	University College Cork	christopherconnor22@outlook.com
Cian	O'Brien	NUI Galway	c.obrien40@nuigalway.ie
Aoife	O'Neill	University of Limerick	aoife.oneill@ul.ie
Denis	Patterson	Dublin City University	denis.patterson2@mail.dcu.ie
Clare	Phalan	University College Dublin	clare.phalan@ucdconnect.ie
Petri	Piiroinen	NUI Galway	petri.piiroinen@nuigalway.ie
Rachel	Quinlan	NUI Galway	rachel.quinlan@nuigalway.ie
Alex	Safar	Cardiff University	SafarAT@cardiff.ac.uk
Aleksandar	Senek	Uppsala Universitet	aleks.senek@gmail.com
Qays	Shakir	NUI Galway	q.shakir2@nuigalway.ie
Eoghan	Staunton	NUI Galway	eoghan.staunton@nuigalway.ie
Shane	Walsh	University College Dublin	shane.walsh.3@ucdconnect.ie
Malgorzata	Wieteska	IT Sligo	s00134694@mail.itsligo.ie
Chun	Xie	University College Cork	chun.xie@ucc.ie